CARDIAC OUTPUT IMPROVEMENT IN MECHANICAL CIRCULATORY SUPPORT DEVICES

A Dissertation
Submitted to the Graduate Faculty
of the
North Dakota State University
of Agriculture and Applied Science

By

Muhammad Bilal Qureshi

In Partial Fulfillment of the Requirements
for the Degree of
DOCTOR OF PHILOSOPHY

Major Department:
Electrical and Computer Engineering

May 2017

Fargo, North Dakota

North Dakota State University
Graduate School

Title

CARDIAC OUTPUT IMPROVEMENT IN MECHANICAL CIRCULATORY SUPPORT DEVICES

By

Muhammad Bilal Qureshi

The Supervisory Committee certifies that this ***disquisition*** complies with North Dakota State University's regulations and meets the accepted standards for the degree of

DOCTOR OF PHILOSOPHY

SUPERVISORY COMMITTEE:

Daniel L. Ewert
Chair

Jacob S. Glower

Kimberly A. Vonnahme

Steven C. Koenig

Approved:

06/14/2017
Date

Alan Kallmeyer
Department Chair

ABSTRACT

Mechanical circulatory support devices (MCSDs) have gained widespread clinical acceptance as an effective heart failure (HF) therapy. The concept of harnessing the kinetic energy (KE) available in the forward aortic flow (AOF) is proposed as a novel control strategy to further increase the cardiac output (CO) provided by MCSDs. A complete mathematical development of the proposed theory and its application to an example MCSDs (two-segment extra-aortic cuff) are presented. To achieve improved device performance and physiologic benefit, the example MCSD timing is regulated to maximize the forward AOF KE and minimize retrograde flow. The proof-of-concept was tested to provide support with and without KE control in a computational HF model over a wide range of HF test conditions. The simulation predicted increased stroke volume (SV) by 20% (9 mL), CO by 23% (0.50 L/min), left ventricle ejection fraction (LVEF) by 23%, and diastolic coronary artery flow (CAF) by 55% (3 mL) in severe HF at a heart rate (HR) of 60 beats per minute (BPM) during counterpulsation (CP) support with KE control. This research also explains how selection of inflation and deflation timing points for extra-aortic two-segmented cuff counterpulsation device (CPD) can affect the hemodynamic of the cardiovascular system (CVS). A comprehensive analysis of compliance profile timings generated through exhaustive search technique and the one selected through steepest descent method is carried out to predict and compare the difference in SV via computer simulation models. The influence of control modes (timing and duration) of deflation and inflation for extra-aortic two-segmented CPD on hemodynamic factors compared to no-assist HF were investigated. Simulation results ($P < 0.05$) predicted that the two-segmented CPD with *late deflation and early inflation* mode would be a suitable mode with 80% augmentation in peak diastolic aortic pressure (AOP), reduction in peak systolic pressure up to 15%, increases in CO by 60% and mean CAF by 80%. The proposed KE

control concept may improve performance of other MCSDs to further enhance their potential clinical benefits, which warrants further investigation. The next step is to investigate various assist technologies and determine where this concept is best applied.

ACKNOWLEDGEMENTS

First of all, thanks to ALLMIGHTY ALLAH Who has helped me during the course of my studies. All my knowledge, strength, health, courage, and abilities are His blessings upon me and there is no way to fulfill His right to thank Him.

Special thanks to Dr. Daniel L. Ewert, my advisor, for his help, innovative ideas and guidance. I offer my sincere and deep hearted gratitude to my advisor who always encouraged me, and determinedly conveyed the spirit and guidance essential for the research. Without his continuous efforts and kind guidance, this disquisition would not have been possible.

Special thanks to my committee members, Dr. Jacob S. Glower, Dr. Kimberly Vonnahme, and Dr. Steven C. Koenig for their support, guidance and cooperative recommendations. I would like to appreciate Dr. Benjamin Braaten efforts for providing me funding opportunity on UAS project that helped me a lot to cover up my financial expenses and I am also very thankful to all the team of UAS project.

Thanks to the Electrical and Computer Engineering staff members Laura D. Dallmann, Jeffrey Erickson, and Priscilla Schlenker for their help and favor.

I would also like to thank my family. Their continuous support is always a source of encouragement and motivation for me.

Finally, I pay my heartiest thanks to all my friends and colleagues here in the US and Pakistan, who always helped me in the time of need.

DEDICATION

I would like to dedicate this thesis to my family, especially to my parents, teachers, and my friends for their love, motivation, and support.

TABLE OF CONTENTS

LIST OF TABLES

LIST OF FIGURES

LIST OF ABBREVIATIONS

ACC .....American college of cardiology

AHA.....American heart association

AOF.....Aortic Flow

AOP.....Aortic Pressure

BiVAD .....Biventricular assist device

BNP.....Brain natriuretic peptide

BPM .....Beats per minute

CAF.....Coronary artery flow

CBF .....Coronary blood flow

CHF.....Congestive heart failure

CO .....Cardiac Output

$CaO_2 – CvO_2$.....Arterial-venous oxygen difference

CPD.....Counterpulsation device

CRT.....Cardiac resynchronization therapy

CS.....Cardiogenic shock

CT .....Computed tomography

CVS.....Cardiovascular system

DET.....Deflation end time

DPA.....Dynamic pressure area

DST .....Deflation start time

EAB.....Extra-aortic balloon

ECG.....Electrocardiogram

ECP .....Enhanced external counterpulsation

ED-EI .....Early deflation and early inflation

ED-LI .....Early deflation and late inflation

EDP .....End diastolic pressure

EDPVR .....End diastolic pressure volume relationship

EDV .....End diastolic volume

EF .....Ejection fraction

ESP.....End systolic pressure

ESPVR .....End systolic pressure volume relationship

ESV .....End systolic volume

FDA.....Food and drug administration

HF .....Heart failure

HR .....Heart rate

IABP .....Intra-aortic balloon pump

IC.....Ischemic cardiomyopathy

IDC.....Idiopathic dilated cardiomyopathy

IET .....Inflation end time

IST.....Inflation start time

KCV .....Kantrowitz CardioVAD

KE .....Kinetic energy

LA .....Left atrium

LAP .....Left atrium pressure

LD-EI .....Late deflation and early inflation

LD-LI .....Late deflation and late inflation

LV .....Left ventricle

LVAD .....Left ventricle assist device

LVEF.....Left ventricle ejection fraction

LVEP.....Left ventricle ejection pressure

LVP.....Left ventricle pressure

LVV.....Left ventricle volume

MAP.....Mean arterial pressure

MCS.....Mechanical circulatory support

MCSD.....Mechanical circulatory support device

MI.....Myocardial infraction

NYHA.....New York heart association

PACD.....Para-aortic counterpulsation device

PAD.....Percutaneous access device

PIL.....Percutaneous interface lead

PULVAD.....Pressure unloading left ventricle assist device

PV.....Pressure volume

RV.....Right ventricle

SV.....Stroke volume

TCM.....Tokotsubo cardiomyopathy

VAD.....Ventricular assist device

LIST OF SYMBOLS

R_M .....Mitral valve internal resistance

P_M.....Opening pressure of mitral valve

R_A.....Aortic valve internal resistance

P_A .....Opening pressure of aortic valve

R_C .....Coronary arteries resistance

L_S.....Blood inertance in aorta

R_S .....Systemic circulation resistance

C_S .....Systemic circulation compliance

E(t) .....Time varying elastance

C(t) .....Time varying compliance

V_0 .....Dead volume in left ventricle

E_{min}.....Minimum elastance of left ventricle

E_{max} .....Maximum elastance of left ventricle

t .....Time variable in seconds

μ .....Cardiac cycle mean

σ .....Cardiac cycle deviation from mean

$C_{Cuff}(t)$ .....Time varying compliance of proximal cuff

L_{Cuff} .....Inertance of blood in proximal cuff

R_{Cuff}.....Resistance of proximal cuff

l .....Length of proximal cuff

r .....Outer radius of proximal cuff

ρ .....Blood density

d1.....Deflation time search direction

d2.....Inflation time search direction

area1 ..... Area of downstream aortic flow calculated on initial inflation and deflation points

area2 ..... Area of downstream aortic flow calculated after time shift in deflation time

area3 ..... Area of downstream aortic flow calculated after time shift in deflation time

shift ..... Small value of time shift in inflation and deflation

T1max ..... Maximum value of deflation time

T1 ..... Initial value of deflation time

T2max ..... Maximum value of inflation time

T2 ..... Initial value of inflation time

step size ..... Maximum allowable step change in inflation and deflation time

f1 ..... Function to calculate step size b

f2 ..... Function to calculate step size c

a0 ..... First step size

d0 ..... Last step size

a, b, c, d ..... Step sizes

P ..... Optimal step size

v ..... Velocity of the blood flow

Area ..... Area of aorta

$Flow_{in}$ ..... Blood flow into the proximal cuff

$Flow_{out}$ ..... Blood flow out of the proximal cuff

v(t) ..... Blood volume in the proximal cuff

1. INTRODUCTION

1.1. Heart Failure

Heart failure (HF) is a challenging clinical condition described by reduction of blood in ventricles either filling or ejection due to various cardiac disorders [1]. In high income countries, the incident of HF is one of the major unsolved healthcare concern challenging medical professionals nowadays. HF is a real epidemic, liable for 5% of hospitalization globally and is the leading cause of hospitalization in the United States affecting more than five million patients with approximately 670,000 new cases diagnosed annually [1]–[6]. HF, in its severe forms, can be remarked as two deadly clinical entities: (1) end-stage chronic HF, with less than a year mortality of approximately 80% which is even worse than many cancer types [7]; and (2) acute HF with cardiogenic shock (CS) with post-myocardial infraction (MI), CS mortality rates nearly approaching 50% [8].

With modern management of cardiac disorders, quality of life of HF patients has improved and more patients are living. Despite significant improvement in development of pharmacologic and device related therapy including cardiac resynchronization therapy (CRT) for HF treatment, majority of patients eventually deteriorate to the level where they required the used of advanced cardiac therapies such as mechanical circulatory support (MCS) or heart transplant. Heart transplant is the gold standard for end-stage HF and offers the best chance for long-term survival but is limited by the donor heart shortage (~2500) and cannot meet the growing demand (up to 100,000 per year) [9], generating a necessity for effective therapy with short- or long-term, partial or full MCS that can improve functional capacity, quality of life, and survival of these patients [10].

1.1.1. Acute Heart Failure Recovery

Any acute or severe dysfunction of left ventricle (LV) or right ventricle (RV) may possibly lead to CS. However, in most cases the primary reason of CS is LV dysfunction resulting in an acute MI [11]. Although, the fact that the majority of these patients undergo ST elevation MI, CS also take place in about 2.5% of non-ST elevation MI [12]. In addition to this mechanical complications like ventricular septal rift, severe spewing in mitral valve and wall rift may result in CS and probably expected in patients with CS obscuring non-anterior MI [13]. Other rare causes may comprise of acute pericardial inflammatory syndrome, isolated failure of RV, transient cardiac syndrome also known as Takostsubo cardiomyopathy (TCM), acute valvular spewing, hypertrophic cardiomyopathy (heart muscles becomes abnormally thick), excess beta, dilated cardiomyopathy (heart ability to pump more is decreased), cardiac tamponade (compression of the heart caused by fluid gathering in the sac surrounding the heart), perioperative low cardiac output (CO) syndrome, and cardiac catheterization difficulties related with CS [14].

The treatment objective (or recovery) of acute HF, is hemodynamic support during cardiac disintegration, involving actions that allow the incapacitated myocardium to recover and overcome the necessity for acute support [15].

1.1.2. Chronic Heart Failure Recovery

The treatment objective of cardiac restoration is a deadly component of HF development linked with poor diagnosis [16], [17] consisting of cellular, molecular and interstitial changes, demonstrated clinically as variations in shape, size, and function of the heart resulting in cardiac injury [18]. Critical variations at the organ level consist of alteration in LV geometry [19], [20], thinning of LV wall [21], increase in LV end-diastolic volume (EDV) and end-systolic volume (ESV), and consequent decrease in ejection fraction (EF) of LV [22]. Molecular and cellular

variations constitute of myocyte hypertrophy, shortage of myocytes because of necrosis (which usually activates with an impairment of the cell's capacity to maintain homeostasis to an influx of water and extracellular ions) [23] or apoptosis (in contrast to necrosis, it is a way of cell death that happens under normal physiological conditions and the cell is an active member in its own demise) [24], fibrosis fibroblast [25], and proliferation [26].

The goal of chronic HF treatment is to improve indications and quality of life, which can be attained by prevention of the critical mechanisms of LV restoration and reversal of already completed LV restoration. As of today, we are aware of the fact that any level of reverse LV restoration is linked with an equivalent increase in the survival of patients suffering from HF [27].

According to Kontogiannis et al. 2016 cardiac surgeons introduced the term "bridge to transplantation" for the patients with chronic HF undergoing mechanical assistance with left ventricular assist device (LVAD), because of the unavailability of the donor heart at the time of heart transplantation. Consequently, the term "recovery" for chronic HF refers to persistent reversal of the above-mentioned variations, a procedure known as reverse remodeling with near stabilization of the LV functions in patients on LVAD followed by a "safe" LVAD implantation. In other words the LV recovery assumes that the patient can survive a big cardiac operation for implantation of LVAD and remain stable afterward both clinically and hemodynamically [28]. However, this assumption does not apply to patients on MCS device that is easily implantable and like the percutaneous intra-aortic balloon pump (IABP). For example, one of the patients of Kontogiannis et al. with chronic HF because of idiopathic dilated cardiomyopathy (IDC) needing MCS by IABP. They found that after 3 months of continuous support, the patient was successfully stopped from the assistance and after 5 years there was no symptoms of HF. Moreover, the patient didn't have to go through a major cardiac surgery to remove the device, which could be the reason

he did so fine. The patient mentioned in the study is now 25 years old and he had a past record of gradually worsening HF when he was first diagnosed at age 21 with IDC complicated by CS, a left ventricle ejection fraction (LVEF) of 17%, brain natriuretic peptide (BNP) of 2800 pg/mL. The patient was placed on IABP support although he had the option of biventricular assist device (BiVAD), he preferred support with IABP. After 3 months IABP improvements in LVEF = 25% and BNP = 207 pg/dL allowed to stop IABP support, and later 5 years LVEF = 30% and VO_2peak = 29 mL/kg per minute without any support [28].

Kontogiannis et al. also concluded that patients who undergo safe and easy MCS to implant (like IABP which is a counterpulsation device (CPD)), the support can be terminated for myocardial recovery when the conditions (Table 1) are met. However, for LVADs implantation required complicated surgery, the recovery can only be considered if the conditions (Table 1) are satisfied [28].

Table 1. Conditions of recovery with easily implantable CPDs and continuous flow LVADs.

CPDs	
Ejection fraction	5%↑
Brain natriuretic peptide	< 500 pg/dL
Continuous flow left ventricle assist devices	
Left ventricle end- diastolic dimension	< 60 mm
Left end-systolic diameter	< 50 mm
Ejection fraction	> 45%
Left ventricle end-diastolic pressure	< 12 mmHg
Cardiac index (resting)	> 2.8 L/min per square

1.2. Counterpulsation Devices for Myocardial Support

Myocardial support with counterpulsation devices (CPDs) is the earliest and most common form of MCS. In past four decades, counterpulsation by IABP has been successfully and widely used for short-term treatment. Every year worldwide more than 160,000 patients receive this

treatment, and with a very promising successful clinical rate of 43% to 65%. IABP is often used for CS or severe LV dysfunction following heart surgery [29]–[32].

Counterpulsation was initially presented in early 1950's when Kantrowitz et al. verified augmentation of coronary blood flow through increase in diastolic pressure [33]. Later in 1959, he added that diaphragm contraction wrapped around the descending thoracic aorta during diastole managed to reduce the LV stress. Other long-term counterpulsation approaches tried involved IABP through a synthetic graft attached to left subclavian artery [34], a descending aortic patch sewn into the descending thoracic aorta, and by wrapping the pedicle latissimus dorsi muscle around the aorta. However each of these approach has its limitations [35].

The hemodynamic advantages of counterpulsation therapy in patients with acute cardiac dysfunction is the major reason using IABP as an effective temporary MCS device. In 1962, Moulopoulos et al. developed the IABP [36], which was implanted in human subject 6 year later for the management of post MI CS [35]. Since then IABP has been widely used in patients with CS, those waiting for advanced cardiac care, and those undergoing coronary artery bypass surgery [34]. However, the application of long-term IABP counterpulsation in the setting of chronic HF remains incomplete; the prospective of long-term counterpulsation may be improved by implementation of novel, fully implantable CPDs. With the recent mission for more effective, smaller and long-term MCSDs, a number of other CPDs have been under examination [10]. These CPDs include the para-aortic counterpulsation device (PACD) [37], representing the early version of the pressure unloading LVAD (PULVAD) named Kantrowitz CardioVAD (KCV) (LVD Technology, Detroit, MI) [38], the Symphony device (Abiomed (Danvers, MA) and SCR (Louisville, KY)) [9], [39], and C-Pulse (Sunshine Heart Inc., Eden Prairie, MN) [40].

1.3. Dissertation Outline

The dissertation is organized as follows. In Chapter 2, we present the background and related literature. Chapter 3 presents a novel idea to improve cardiac output of mechanical circulatory support devices by optimizing kinetic energy (KE) available in forward moving aortic blood flow. Chapter 4 presents optimal timing control of extra-aortic two-segmented counterpulsation device using exhaustive search mechanism.

2. RELATED WORK

2.1. Counterpulsation Theory of Application

The main functionality of any counterpulsation therapy is to augment the aortic pressure (AOP) during the native heart diastole with the use of mechanical circulatory support device (MCSD) to achieve an increase in coronary artery flow (CAF) known as myocardial perfusion as well as decreases AOP during native heart systole to achieve reduction in ventricle afterload and external work [41]. There are numerous CPDs in clinical use and in development phase that work on the above-mentioned principle. For example, an IABP placed in the descending aorta inflates a balloon with bursts of shuttle gas during native diastole pushing blood to the heart, and deflates the balloon before the native heart systole, and deflates the balloon just before the native heart systole thus reducing the AOP. Likewise, Symphony device achieves similar effects by displacing the blood and C-Pulse by squeezing the aorta. The effectiveness of the Counterpulsation therapy rely generally on the control algorithms, i.e. the timing and synchronization of the device to native cardiac beat, which is usually accomplished with the help of electrocardiograph (ECG) or AOP waveform to trigger the device for inflation and deflation. Generally, the ECG waveform is used to detect R-wave to find out the beginning of the ventricle systole however, AOP waveform can be used to observe the placement, timing, and efficacy of the counterpulsation therapy by calculating the peak diastolic and end-diastolic pressure (EDP) as shown in Figure 1.

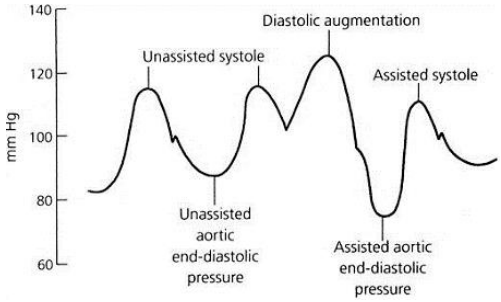

Figure 1. Effect of assistance with counterpulsation on AOP waveform during diastole and systole [42].

In order to account of time delays finer adjustments in CPD timing can be made manually for optimization [42].

2.2. Physiological Benefits of Counterpulsation

Counterpulsation therapy offers great clinical advantages for the heart, end organs and peripheral circulation for the patients with myocardial dysfunction. Reduces the ventricle afterload and external work because of the decreased ventricle pressure. Counterpulsation therapy increases the diastolic AOP by 30% to 70% and provide significant improvement in coronary perfusion [29], [43], [44].The peak systolic pressure is reduced by 5-15%, while EDP is decreased up to 30% [29], [31], [45]. Counterpulsation therapy also reduces native heart rate (HR) by 10% [30] and may reduce LV EDV up to 10 to 15% [46]. Counterpulsation improves oxygen supply to heart through increased coronary perfusion and decrease oxygen consumption by reducing ventricle afterload and external work [30], [47], [48]. Counterpulsation increases CO and stroke volume (SV) up to 20% [43], [49]. Counterpulsation therapy also helps in improving metabolic function and in regaining of end organ functions [30] e.g. cerebral, renal, mesenteric and pulmonary blood [50]–[53]. Table 2 lists the summary of hemodynamic and metabolic benefits of Counterpulsation therapy.

Table 2. Summary of counterpulsation therapy hemodynamic and metabolic benefits.

Hemodynamic Benefits		Metabolic Benefits	
Coronary Perfusion	↑ 0 to 100%	Myocardial Oxygen Consumption [54] $MVO_2 = CBF \times (CaO_2 - CvO_2)$	25% ↓
Diastolic AOP	↑ 30 to 70%	Myocardial Oxygen Supply	↑
LV Peak Systolic Pressure	↓ 5 to 15%	End Organ Perfusion	↑
LV End-Diastolic Pressure	↓ 5 to 30%		
HR	↓ 0 to10%		
LV EDV	↓ 5 to 15%		
CO	↑ 0 to 20%		

Counterpulsation therapy is very effective in patients with HR between 80 to 110 BPM [55], [56], systolic AOP between 40 to 70 mmHg [57], and have high arterial stiffness [58]–[60]. Optimal preformation of counterpulsation is gained when its volume is equal to the SV of LV [61]and is effective as close the device is near to aortic wall. However, due to minor risk of obstruction or embolization to the aortic vessels CPDs are usually positioned at three different locations 1) IABP is implanted in the descending aorta and 2) Symphony device near to axillary artery and C-Pulse around the ascending aorta.

2.3. Types of Counterpulsation Devices

2.3.1. Extracorporeal Counterpulsation Devices

Enhanced external counterpulsation (ECP) technique is used to provide non-invasive extracorporeal counterpulsation therapy. During ECP pneumatic cuffs placed externally on patient lower extremities are inflated and deflated. Mostly ECP (Figure 2) is performed by placing three cuffs on each leg i.e. on the upper thighs, lower thighs and the calf and like every counterpulsation the inflation and deflation is ECG triggered (R-wave detection). During deflation period of cycle, the upper thighs cuffs deflate first, then the lower thighs and lastly the calf cuffs and in inflation the sequence is reversed. A pressure monitor is used to control the inflation pressure and the cuffs are inflated up to 300 mmHg. ECP has shown to be effective in providing relief to angina, reducing the level of ischemia in a cardiac stress test, improving exercise tolerance and improving CO for HF patients. ECP is recommended for patients who have symptoms of ischemic cardiomyopathy (IC) but are not willing to go for coronary artery bypass surgery. It is not recommended for patients with severe peripheral vascular disease, aortic insufficiency, significant artery disease, aortic insufficiency, uncontrolled hypertension, phlebitis, deep vein thrombosis, bleeding diathesis and stasis ulcers.

Figure 2. Non-invasive counterpulsation therapy with series of cuff placed externally on patient lower extremities to provide ECP for reducing afterload and increasing CO [42].

2.3.2. Percutaneous Counterpulsation Devices

2.3.2.1. Intra-aortic balloon pump

As explained earlier, the hemodynamic and metabolic advantages of the counterpulsation therapy in patients suffering from acute and chronic HF led to the development of IABP MCSD. IABP consist of a polyethylene balloon that is placed in the aorta about 0.8 inches away from the left subclavian artery. The inflation and deflation is performed by shuttling helium gas in the balloon [10].

IABP is recommended for the patients experiencing CS, reversible mechanical cardiac complications following MI, post craniotomy failure, angina pectoris, injury to myocardial tissue, substantial risk coronary artery bypass surgery, preoperative use for patients with unstable angina with stenosis greater than 70% of main coronary artery, LV dysfunction (LVEF < 35 %). IABP is not recommended for patients with severe aortic valve insufficiency and aortic dissection. Relative

contraindications are prosthetic vascular aortic grafts, aortic aneurysm, and aortofemoral grafts. IABP is a blood contacting device hence required anticoagulation regimen with heparin [42].

IABP is a short-term counterpulsation this is implanted in the descending aorta (Figure 3) using a percutaneous access to the femoral artery into descending aorta, and therefore requires patient to supine during the course of therapy. The location of an IABP in descending aorta and biocompatibility issues do not allow IABP to be used for longer period typically (> 14 days) [62], [63]. Prolonged support of IABP results in increased vascular complications, bleeding and infection [63], [64]. Timing of IABP inflation and deflation plays an important role to make sure balloon doesn't block the aortic flow (AOF) therefore, IABP needs to be rapidly deflated before the ventricle ejection starts [65], and this rapid deflation causes retrograde flow restraining the maximum hemodynamic and metabolic advantages of IABP counterpulsation. Recent technological advancement greatly refined the IABP counterpulsation and now it consists of sheath less insertion technique, smaller sizes of balloon catheter and optical fiber based pressure sensors. The revised insertion and advanced pressure sensor enabled improved distal limb perfusion by reducing the outer diameter lumen of the IABP catheter. The variety of balloon sizes allows surgeon to select the balloon that better match patient internal diameter and height of the aorta.

Given the limitations of IABP and proven hemodynamic and metabolic advantages of counterpulsation, several new CPDs are being developed for long-term therapy, including (Kantrowitz CardioVAD, Symphony device and extra-aortic C-Pulse). These CPDs provide long-term support of chronic HF along with implantation system and are less invasive than current ventricular assist devices (VADs). Like IABP all these CPDs provide improved coronary artery perfusion and reduce ventricle workload.

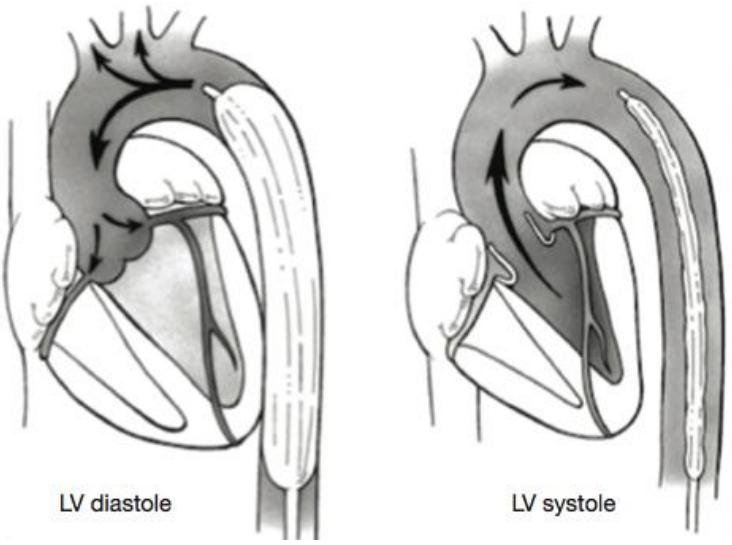

Figure 3. IABP placed in the descending aorta, timed to inflate during diastole to augment the coronary perfusion and deflate during systole before the onset of ventricular ejection to decrease the LV afterload and external work [66].

2.3.3. Modern Implantable Counterpulsation Devices

2.3.3.1. The Kantrowitz CardioVAD

Kantrowitz CardioVAD (KCV) is a chronic MCSD (currently in clinical trials) designed (by LVAD Technologies Detroit, MI) to provide long-term assistance to severe to moderate HF patients. This CPD is designed especially for the patients who are unable to qualify for heart transplant but still have some cardiac function. This device delivers systolic unloading and diastolic augmentation of the failing heart.

This device (Figure 4) is pneumatically driven and consists of Cardioplus pump (60 cc), percutaneous access device (PAD), and a wearable unit for control and has a similar physiological function to IABP. The CardioPlus pump weighs less than an ounce and is approximately 6.5 inches in length [42]. The Cardioplus pump is surgically implanted in the descending aorta with patient on cardiopulmonary bypass which increase the risk of morbidity and mortality.

This device is a non-obligatory and can be turned on/ off for minutes or hours from external unit when the patient's wishes without the increasing risk of thromboembolism. Patients on this

device showed immediate and sustained major improvements in exercise capacity [38], [66], [67]. However, this device can't be implanted in patients experiencing severe biventricular dysfunction and uncontrolled tachyarrhythmia [38].

Figure 4. Illustration of Cardioplus patch surgically implanted, to provide counterpulsation the patch inflates during diastole and deflates during systole by a wearable pneumatic driver [42].

2.3.3.2. Symphony device

The Symphony device (currently in pre-clinical trials) designed by Abiomed (Danvers, MA) and SCR (Louisville, KY) to fit comfortably in a pacemaker like pocket. It consists of 30 mL SV polyurethane-lined pumping chamber placed in the right side [9], [68] of a patient and a percutaneous driveline that runs form pumping chamber and exists the skin and connects to an external pneumatic driver (weighs about 2.2 kg can be carried or worn on belt). A relatively simple procedure (surface surgical implantation) is required for chamber implantation, the pumping chamber is connected to the systemic circulation by a short graft anastomosed to the right artery.

The Symphony device ejects blood into the circulation during diastole to provide diastolic augmentation and coronary perfusion, and during systole the air is evacuated from the pumping

chamber by the driver thus removing blood from the circulation and reducing external work. The timing of the Symphony device filling and ejection was adjusted to maximize the performance.

Pre-clinical studies have revealed that this device provides superior hemodynamic and metabolic advantages compared to a 40 mL IABP [9], [39], [68]–[71].

This device is typically recommended for patients with NYHA class IIIB and IV HF recovering from acute MI or with chronic angina. However, this device is not recommended for patients with end-stage HF, aortic insufficiency, severe hypertension, infection, severe vascular disease and tiny or blocked axillary or brachiocephalic arteries [10].

This is a blood contacting device therefore requires anticoagulation regimen of initial Heparin in the immediate postoperative period which shifts to chronic Warfarin and antiplatelet therapy with Plavix [42].

2.3.3.3. C-Pulse

The C-Pulse (currently in clinical trials) is an implantable extra-aortic counterpulsation device, designed by Sunshine Heart Inc., Eden Prairie, MN to provide permanent, long-term, continuous and or on-demand partial MCS for class III and ambulatory class IV HF patients. The C-Pulse system includes non-blood contacting (first of its type), ECG-trigged, pneumatically driven, implantable cuff (consisting of balloon and combination wrap) linked to an air tube; a bipolar epicardia ECG sensing lead (attached to RV outflow tract) for transmitting the signals from heart to C-Pulse controller; and a wearable external AC-powered control unit [72].

The C-Pulse cuff consists of a polyurethane balloon and polyester covering designed to follow to the ascending aorta as shown in Figure 5. The air tube and ECG sensing lead passes internally through the abdominal wall and is linked to the external drive unit (which pumps air in and out of the balloon for inflation and deflation synchronized to heart beat). The external unit is

programmable and adjustments can be made in inflation and deflation rate as well as an inflation volume. The C-Pulse cuff inflates inwardly producing a “thumb printing” bend of the outer curvature of the ascending aorta as shown in Figure 5. Depending upon the cuff size and aortic diameter approximately the cuff can displace 20 to 30 mL of blood volume per beat. The C-Pulse balloon is inflated at the closure of aortic valve, which represents the time when the dicrotic notch appears in the AOP waveform and is deflated at the onset of R-wave on the ECG, which take place before the opening of the aortic valve. The device is implanted through median sternotomy [72], requiring a short 15 to 20 minutes implantation procedure and total operation time is approximately between 60 to 90 minutes.

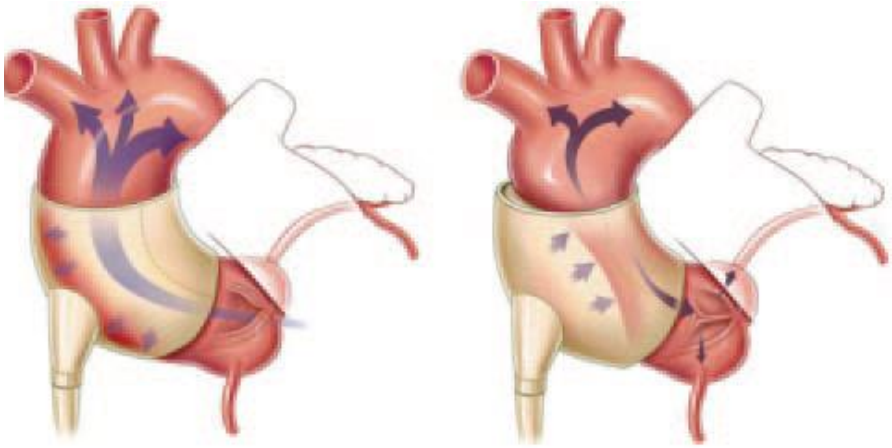

Figure 5. Extra-aortic balloon wrapped around the ascending aorta (deflated (right) and inflated (left) showing thumb print effect [74].

2.4. Exploring Extra-Aortic Balloon (C-Pulse)

2.4.1. Research Studies on Extra-Aortic Balloon Counterpulsation (C-Pulse)

Davies et al. compared the effects of extra-aortic balloon (EAB) counterpulsation with IABP [41]. An EAB with 17 mL volume around the ascending aorta compared to IABP with a balloon volume of 25 mL in the descending aorta. Measurement of arterial and central venous pressures, flow in coronary and descending aorta at baseline and after EAB or an IABP using (1:1)

and (1:2) modes were performed. During (1:1) mode baseline data was compared with EAB and IAB, and during (1:2) mode assisted beat data was compared and analyzed with unassisted beat.

The results of Davies et al. suggested that both the CPDs augmented the peak diastolic pressure and decreased the LV afterload. EAB counterpulsation was found to increase diastolic CAF in both modes by 69% in (1:1) and by 63% in (1:2) assisted versus unassisted beat. IABP significantly increased diastolic CAF by 28% in (1:2) mode. Both devices shown augmentation in total CAF and some increase was observed in AOF as well. This study suggested that EAB could be used as a better option in patients suffering from mild to severe HF because of its non-blood contacting nature and easy implantation.

Later Legget et al. performed a study of EAB in humans [73]. The goal of this was to conclude the safety and performance of EAB in six patents with normal LV function enduring off-pump coronary bypass surgery. EAB was implanted and attached to standard counterpulsation counsel. At baseline with (1:1) and (1:2) modes hemodynamic and echocardiographic parameters of ventricle function and CAF were measured. It was found that systolic, diastolic and venous pressures were comparable to baseline during counterpulsation. However, during (1:1) counterpulsation mode HR fall down from (76 ± 1.2 to 72 ± 1.1, $P = 0.055$) but there was no significant change in HR. However, an increase of 67% in diastolic CAF, 13% improvement in fractional area change and reduction of 6% in end-diastolic area, 16% in end-systolic area and 31% in LV wall stress was reported with EAB (1:1) compared to baseline. EAB also shown 26% rise in velocity of fiber shortening and inverse correlation between wall stress and fiber shortening was observed during EAB (1:1) counterpulsation, representing that EAB improves LV function (velocity of fiber shortening) by decreasing the LV afterload (wall stress). Finally, it was

concluded in this study [73] that EAB augments CAF, decreases afterload, and there were no complications noticed during EAB short-term use 35.

Similarly, Hayward et al. tested C-Pulse on humans to further explore the feasibility, safety, and hemodynamics effects in five severe HF patients (NYHA class III or IV) aged between 54 and 73 years [72]. All the patients shown improvement by one NYHA class, and major hemodynamics improvement were found in three patients. One patient was successfully transplanted after a month, one patient remained on C-Pulse for six months and shown significant improvements in hemodynamics but suffered complications [72]. However, in remaining three patient's infectious complications were developed.

At present, a potential, randomized test to access the safety and efficacy of C-Pulse in patients with NYHA class III or ambulatory class IV HF is in progress. Solanki P reported estimated sample for this study was about 388 subjects (estimated completion is in 2017) and patients were randomized to test and control groups [10]. Food and Drug Administration (FDA) approval to market this device in USA is subject to the demonstration of safety and efficacy of C-Pulse system through this study.

2.4.2. Possible Candidates for Extra-Aortic Balloon Counterpulsation (C-Pulse)

C-Pulse system is an implantable MCSD that is non-blood contacting and non-obligatory for providing short- or long-term, partial or full support for moderate to severe HF patients. According to the studies performed by Davies et al., Legget et al., and Hayward et al. ACC/AHA stage C and NYHA class III or ambulatory class IV patients with LVEF < 35% symptoms despite optimal medical and device related therapies can be considered possible candidates for C-Pulse device. Investigational studies (echocardiography, computed tomography (CT) chest, etc.) are performed before possible candidacy eligibility to eliminate any chronic diseases that can restrict

patients for getting C-Pulse. Timing of candidate selection is very important because once patients move in to NYHA class IV HF, the implantation of C-Pulse system is too late. For the C-Pulse system implantation ascending aortic outside diameter should need to be greater than 28 mm and less than 42 mm [10]. C-Pulse can be implanted if the candidate has mild degree of aortic atheroma and mild aortic spewing.

C-Pulse system implantation is not recommended to patients with moderate to severe aortic insufficiency, ascending aorta calcification, aortocoronary bypass grafts, history of aortic dissection or disorder of other connective tissues to aorta, prior LVAD or heart transplant and ACC/AHA stage D or NYHA non-ambulatory class IV HF patients [10].

2.4.3. Advantages and Disadvantages of Extra-Aortic Balloon Counterpulsation

Extra-aortic balloon counterpulsation is a non-blood contacting device and it does not required anticoagulation hence minimizing the risk of thrombus. It is easily implantable device (wrapped around the ascending aorta), minimally invasive designed to implant without the need of cardiopulmonary bypass and is usually implanted via small incision of the size of pacemaker through the ribs and sternum or through traditional full sternotomy allowing patient to ambulate soon after its implantation. No significant embolic actions reported with the use of this device, since it is non-obligatory CPD it can be disconnected for hours. Moreover it is also reported that diastolic augmentation is more effective at ascending aorta than descending aorta [74]. The deflation of extra-aortic balloon CPD on the anterior of aorta reduces strain and produces no mechanical injury to the aortic wall unlike IABP which forms mechanical injury to endothelium due to the location of its implantation [75].

Extra-aortic devices are contraindicated in patients who had past heart surgeries, severe atherosclerosis of the ascending aorta, aortic insufficiency, significant vascular disease and

coronary artery bypass. Driveline infection remains the most contrary incident in extra-aortic devices [40]. The long-term effect of extra-aortic device on the aortic wall is still unknown, although in an animal model study, the cuff compression indicated only mild inflammatory alteration of the adventitia and normal media and intima of ascending aorta [75]. However, Legget et al. reported acute adverse effects in a human study due to cuff compression [73]. It is also reported that the degree of CO improvement in NYHA class III and ambulatory class IV HF may be insufficient [10].

2.4.4. Improving the Hemodynamics of Counterpulsation Devices

Considering the physiological advantages of CPDs for long-term therapy for acute and chronic HF patients and the short coming of limited improvement in CO for NYHA class III and ambulatory class IV, we proposed the novel idea of improving the CO of MCSDs by harnessing the KE of the forward moving aortic blood flow and used extra-aortic CPD as an example. The next chapter elaborates the mathematical modeling of the proposed system and demonstrates the increase in CO attained from this model.

3. A NOVEL IDEA TO IMPROVE CARDIAC OUTPUT OF MECHANICAL CIRCULATORY SUPPORT DEVICES BY OPTIMIZING KINETIC ENERGY TRANSFER AVAILABLE IN FORWARD MOVING AORTIC BLOOD FLOW

This paper is published in Cardiovascular Engineering and Technology journal and is currently under revision process. This chapter discusses the modeling of two-segmented cuff CPD to optimize the KE available in forward moving aortic blood flow, and compares the hemodynamic improvements with no device and single cuff CPD.

3.1. Introduction

Congestive heart failure (CHF) is a complex condition characterized by reductions in either filling or ejection of blood in the ventricles due to various cardiac disorder [76]. Currently, treatment for CHF begins with medications to increase pumping efficiency of the heart and/or followed by implantable pacing devices, before progressing to MCSDs and heart transplants as the last viable option. MCSDs can work by direct systolic augmentation of the heart, mechanically diverting blood from the LV directly into the aorta or via counterpulsation therapy with diastolic augmentation.

Counterpulsation pumps when the heart is in the diastolic state to increase blood flow and oxygen to the heart. Counterpulsation stops pumping when the heart is in the systolic state to decrease the workload and lessen oxygen demand. MCSDs with extra-aortic counterpulsation enables a minimally invasive, non-blood contacting therapy, in which the device may be implanted without the need for extensive dissection facilitating patient ambulation, and is designed to provide long-term partial circulatory support in HF patients (Figure 6). Improvements in diastolic CAF and reductions in the LV afterload with the extra-aortic CPD have been well-documented in many short-term studies [73]. However, it has also been shown that MCSDs with extra-aortic

counterpulsation may produce retrograde flow during diastole that can reduce the CO and CAF [69]. Overall, CPDs are considered insufficient to meet the needs of NYHA ambulatory class IV HF patients [10].

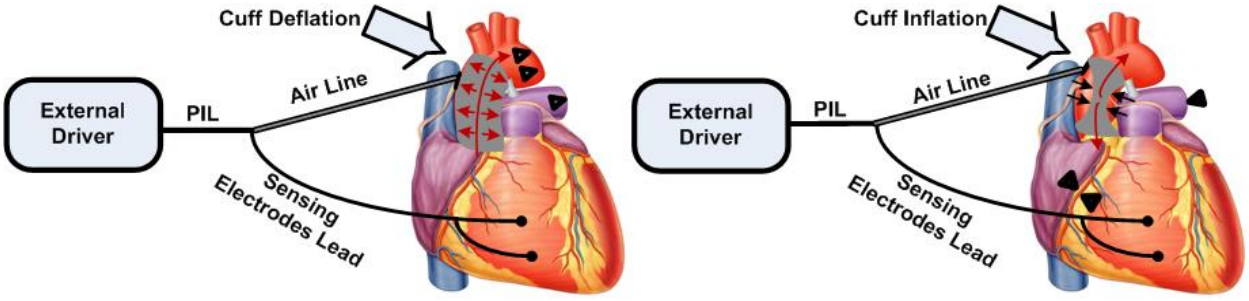

(a) (b)

Figure 6. Illustration of typical CPD consisting of a cuff that is wrapped around the ascending aorta; a bipolar ECG sense lead placed on the left ventricle; an exchangeable wire-wound percutaneous interface lead (PIL) (redrawn from Starck et. al. [77]).

3.2. Materials and Methods

3.2.1. Overview of Cardiovascular System Modeling

A previously reported, a lumped parameter electrical-analog model of the cardiovascular system (CVS) was implemented in Simulink, Matlab 2016 [78]. Single and two-segmented CPD computational models were developed and integrated into the CVS model. The extra-aortic two-segmented cuff CPD was modeled by adding a second cuff of small compliance distal to the single cuff CPD model, and it was controlled by an external timer. Hemodynamic and LV pressure-volume (PV) loops were simulated over a wide range of physiological test conditions mimicking early and late-stage HF. The efficacy of the single and two-segmented extra-aortic CPDs were simulated and compared to quantify CO and characterize retrograde flows.

3.2.2. Electrical Analog Computational Model of the Cardiovascular System

The human circulatory system is divided into a number of lumped parameter blocks in which each block is defined by its own resistance, compliance, pressure, and volume of blood [78],

[79]. Typically, a simplified human circulatory model consists of four valves represented by diodes and six blocks as shown in Figure 7.

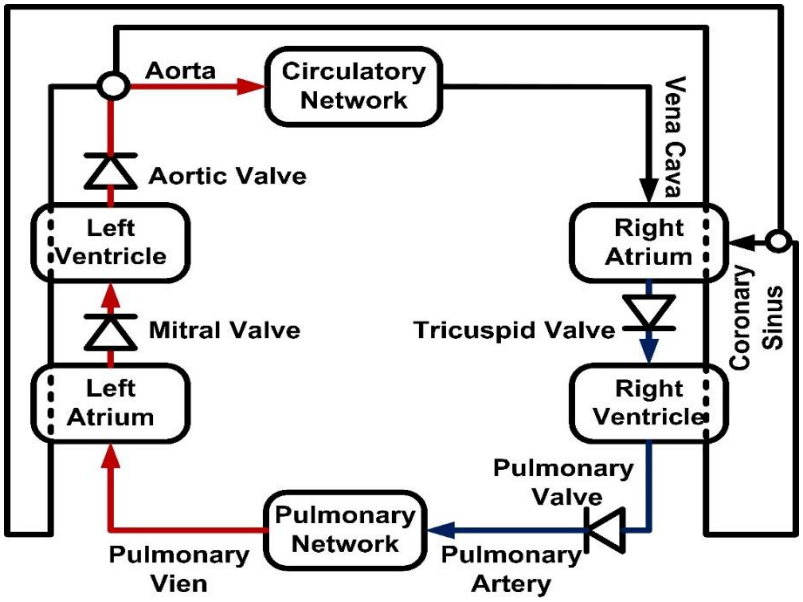

Figure 7. Illustration of human circulatory system.

Among these six blocks, four are considered as active blocks because of their varying compliance. Every block of the model is defined by its resistance (R) to the flow of blood and its compliance (C) which is the capability of a block to store the blood volume (V).

Even though a complete heart model can be appended with a model of assist device, for simplicity we assume that the right heart and pulmonary network are healthy and working under normal conditions. To produce the LV hemodynamics, a second order lumped parameter electrical model of arterial system is developed as shown in Figure 8.

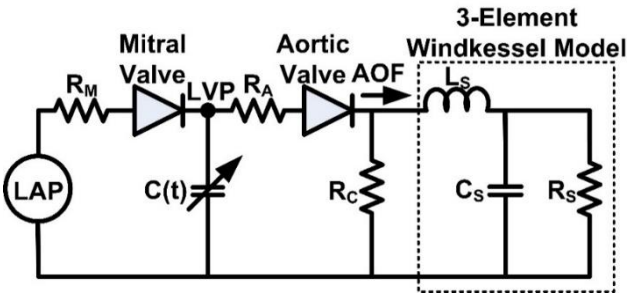

Figure 8. Illustration of lumped parameter electrical equivalent model of the CVS.

In this model, a constant source of 8 mmHg represents the left atrium pressure (LAP), and the mitral valve is represented by a diode that has an internal resistance (R_M) and forward pressure (P_M). The aortic valve is represented by a diode, which also has an internal resistance (R_A) and forward pressure (P_A). Both P_M and P_A are used to simulate the opening pressure of the mitral and the aortic valves. Resistance (R_C) is used to model the coronary arteries of the CVS (so that augmentation of coronary blood flow can be simulated using counterpulsation). The aortic valve is followed by a three element Windkessel model comprised of inductor (L_S), resistance (R_S), and compliance (C_S) for the representation of systemic circulation.

Table 3. Cardiovascular system model parameters for healthy heart.

Parameter	Value	Detail
LAP	8 mmHg	Left Atrium Pressure
R_M	0.0005 mmHg.s/mL	Mitral Valve Resistance
R_A	0.0225 mmHg.s/mL	Aortic Valve Resistance
C(t)	Time-varying	Left Ventricle Compliance
R_S	2 mmHg.s/mL	Systemic Resistance
R_C	4 mmHg.s/mL	Coronary Resistance
C_S	1.5 mL/mmHg	Systemic Compliance
L_S	0.0002 mmHg.s2/mL	Blood Inertia in Aorta
P_M	0.040 mmHg	Forward Pressure of Mitral Valve
P_A	0.080 mmHg	Forward Pressure of Aortic Valve

For model simplicity only three elements have been employed, while maintaining enough complexity to produce the desired LV hemodynamics. Complete details of the CVS model parameters and their corresponding values, [80]–[82] are listed in Table 1.

These values of resistances and compliances differ in different patients; here typical values are used for the LV chamber model. The LV chamber of the heart is modeled as a time varying compliance represented by $C(t)$. The varying compliance $C(t)$ is used since the walls of the heart chambers are elastic and their elastance changes over time through the cardiac cycle. The elastance

function $E(t)$, which is the reciprocal of $C(t)$, describes the relation between the pressure and volume of the LV and is given by the following relation [83].

$$E(t) = \frac{LVP(t)}{LVV(t) - V_0} \tag{1}$$

where $LVP(t)$ represents the LV pressure, $LVV(t)$ represents the volume of the LV, and V_0 is the dead volume of the LV at zero pressure. Various expressions of the LV elastance have been reported [78], [84], [85]. In this study, an exponential function was used, which provides symmetrical responses for the ejection and filling cycles of the heart and can be mathematically represented as:

$$E(t) = (E_{max} - E_{min}) * \exp\left(\frac{(-t - \mu)^2}{2\sigma^2}\right) + E_{min} \tag{2}$$

where E_{max} and E_{min} are the constants representing the maximum and minimum elastance $E(t)$ of the LV and are related to the end systolic pressure volume relationship (ESPVR) and end diastolic pressure volume relationship (EDPVR), respectively. The other constant parameters μ and σ are used to center the mean at ½ of the cardiac cycle and spread the curve to 50% of the duty cycle. A plot of normal LV elastance $E(t)$ with E_{max} = 2 mmHg/mL and E_{min} = 0.06 mmHg/mL is shown in Figure 9.

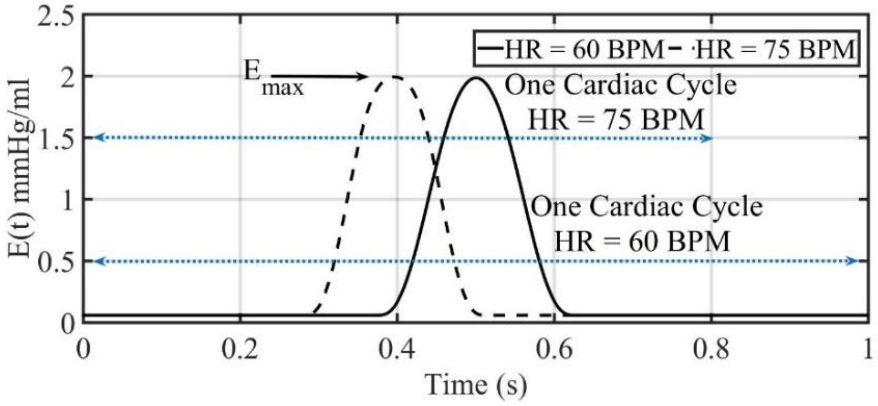

Figure 9. Elastance of LV for normal heart (E_{max} = 2 mmHg/mL) over a period of one cardiac cycle at a HR of 60 and 75 BPM, respectively.

3.2.3. Cardiovascular Model Verification

The capability of the CVS electrical model to match the hemodynamic response of the LV is verified by simulating the model in reaction to changes in parameters. The CVS model is found to be consistent with hemodynamic data in normal heart conditions. Figure 10 shows the simulation waveforms at a HR of (a) 60 and (b) BPM with LV elastance $E(t)$ = 2 mmHg/mL, which corresponds to healthy heart based on its SV and CO. The normal CO range of healthy human heart falls between 4 to 8 L/min.

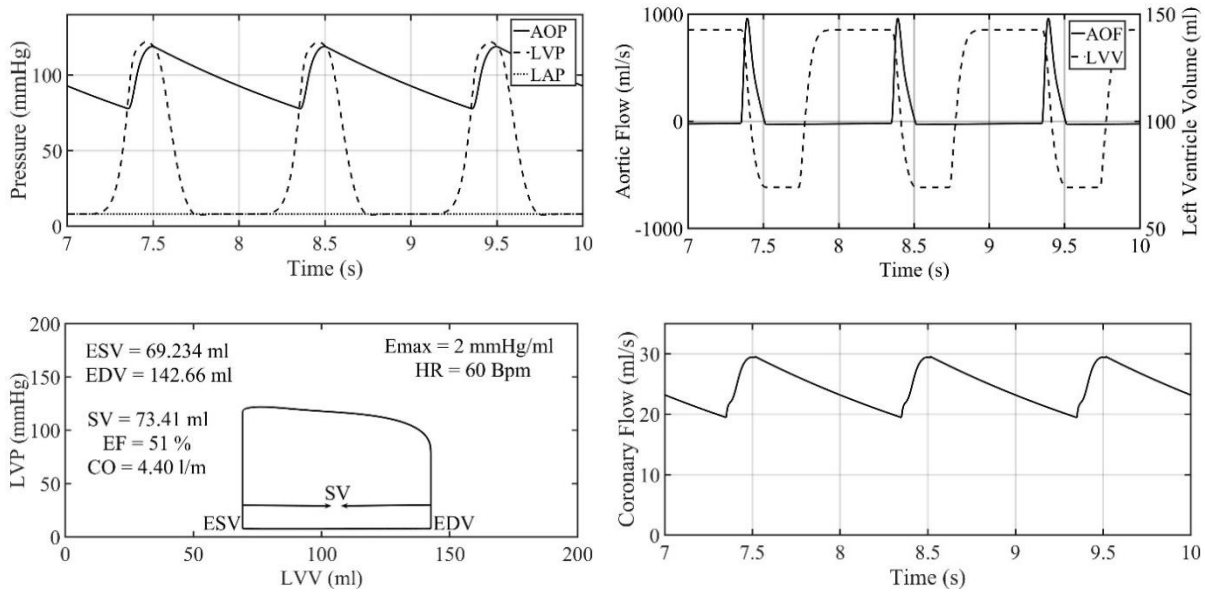

Figure 10. Simulated waveforms of electrical model of the CVS representing the hemodynamic response of normal heart at 60 BPM.

For the specific scenario of 60 BPM with LV elastance $E(t)$ = 2 mmHg/mL as shown in Figure 10, diastolic pressure, systolic pressure, EDV, and ESV are found to be 78.16 mmHg, 118.6 mmHg, 142.7 mL and 69.25 mL respectively under the initial conditions of 120 mL for LVV, 120 mmHg for arterial pressure and 10 mL for LV dead volume. Substituting the values of systolic pressure, diastolic pressure, ESV and EDV in the equations below.

$$SV = EDV - ESV \tag{3}$$

$$\mathrm{CO} = \mathrm{HR} * \mathrm{SV} \tag{4}$$

$$\text{Pulse Pressure} = \text{Systolic Pressure} - \text{Diastolic Pressure} \tag{5}$$

$$\text{Mean Arterial Pressure} = \text{Diastolic Pressure} + \left(\frac{1}{3} * \text{pulse pressure}\right) \tag{6}$$

The pulse pressure calculated is 40.44 mmHg/ml, mean arterial pressure (MAP) is 91.50 mmHg, SV is 73.41 mL/beat and CO is 4.40 L/min.

The model of CVS was further verified by altering the afterload and preload conditions and generating the PV-loop, while keeping the elastance and dead volume of the LV constant at E_{min} = 0.06 mmHg/ml, E_{max} = 2 mmHg/ml and V_0 = 10 mL. Despite the alterations in afterload and preload conditions, linearity between end systolic pressure (ESP) and the LVV (also called ESPVR) validates the behavior of the CVS model similar to the hemodynamic response of the normal LV.

We simulated the afterload conditions for four different values of R_S. The preload conditions were also simulated four different values of R_M. **Error! Reference source not found.** (a) and (b) show the PV-loop for varying afterload and preload conditions with linearity in the ESPVR at a HR of 60 BPM and for E_{max} = 2 mmHg/mL.

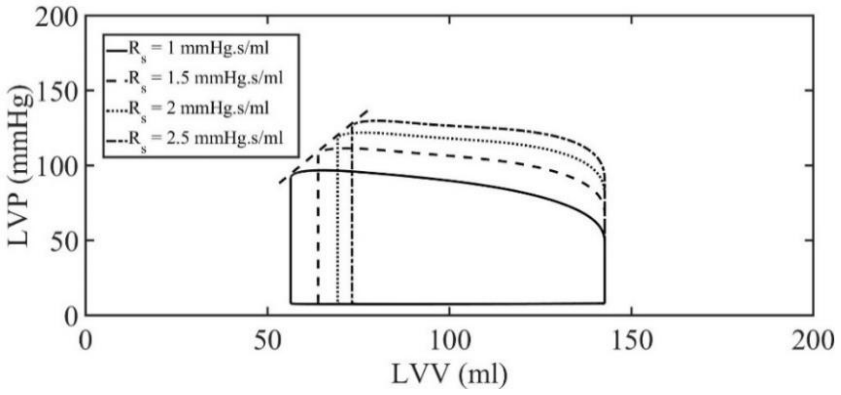

(a)

Figure 11. Linearity of ESPVR in response to alterations in afterload and preload conditions of CVS model are shown in (a) and (b), respectively.

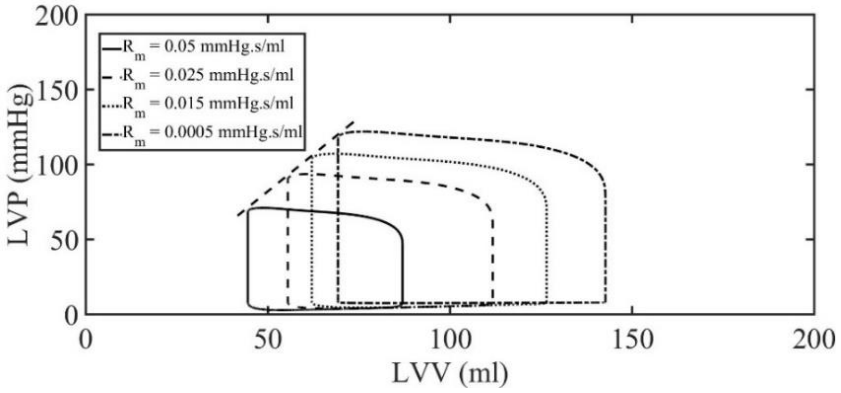

(b)

Figure 11. Linearity of ESPVR in response to alterations in afterload and preload conditions of CVS model are shown in (a) and (b), respectively (continued).

3.2.4. Simulating Heart Failure

A wide range of HF scenarios was simulated ranging from mild to severe (Table 4). The level of HF is represented by the stiffness of the LV muscle [86] the patient's activity level by adjusting R_S, and variations in the HR from 60 to 75 BPM.

Table 4. Heart failure scenarios for 60 and 75 BPM [87].

HR (BPM)	Systemic Resistance (mmHg.s/mL)	Activity Level	E_{max} = 1.00 (mmHg/mL)	E_{max} = 0.75 (mmHg/mL)	E_{max} = 0.50 (mmHg/mL)
60	2.00	Inactive	Mild HF	Moderate HF	Severe HF
75	1.75	Active	Mild HF	Moderate HF	Severe HF
120	1.00	Very Active	Mild HF	Moderate HF	Severe HF

3.2.5. Modeling the Extra-Aortic Single Cuff CPD

The extra-aortic single cuff CPD is modeled with three elements: (1) time-varying compliance ($C_{cuff}(t)$, Equation (7)), (2) inductance (L_{cuff}, Equation (8)) representing the inertia of blood, and (3) a small internal resistance to model the frictional losses. In this model, the CPD displaces 10 to 30 mL of blood volume per cardiac beat [87], and has a length l = 8 cm with an outside radius r = 2.82 cm, which varies depending on the cuff size [40].

$$C_{cuff}(t) = \frac{dV(t)}{dP(t)} \tag{7}$$

$$L_{cuff} = \frac{\rho l}{\pi r^2} \tag{8}$$

The capacity of the extra-aortic single cuff CPD was limited to a maximum of 30 mL using a compliance that is dependent on the AOP. This corresponds to a piece-wise linear CPD pressure-volume relationship where at low pressures the compliance will be higher and at high pressures the compliance will be lower. The maximum cuff compliance will be 0.85 mL/mmHg (severe HF) and 0.45 mL/mmHg (mild HF) for cuff pressures of 35 and 60 mmHg, respectively using Equation (7) (Table 4. Heart failure scenarios for 60 and 75 BPM [87]. An inductance value of 0.003 $\text{mmHg.}\,s^2/\text{mL}$ was obtained by substituting the length and radius of the cuff (Figure 12(a)) and blood density (ρ) of 1.06 gm/cm^3 in Equation (8). The electrical-analog model of extra-aortic single cuff CPD (Figure 12(b)) and its time-varying compliance function were used (Figure 13(a)) for HR of 60 and 75 BPM respectively. The cuff compliance was varied from 0.45 to 0.85 mL/mmHg to limit the maximum filling volume to 30 mL/beat as shown in (Figure 13(a)). The saturation of maximum cuff compliance of 0.85 to 0.45 mL/mmHg (Figure 13(b)), which were obtained using the saturated compliance profile, are the same as unsaturated compliance.

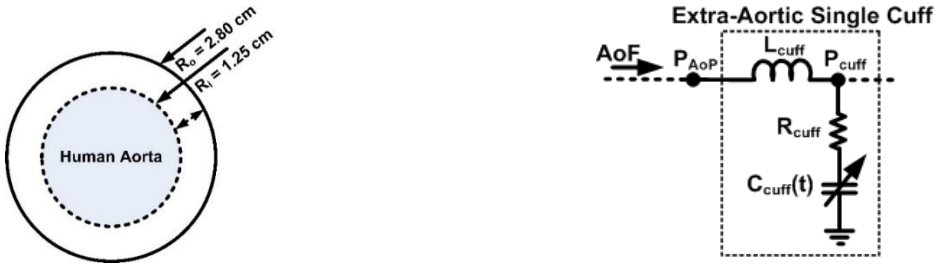

(a) (b)

Figure 12. A geometrical representation of cuff and its electrical equivalent (a) shows inner and outer dimension of a typical extra-aortic cuff wrapped around the aorta and (b) shows the electrical equivalent model of extra-aortic single cuff consisting of time-varying compliance, inductance, and resistance.

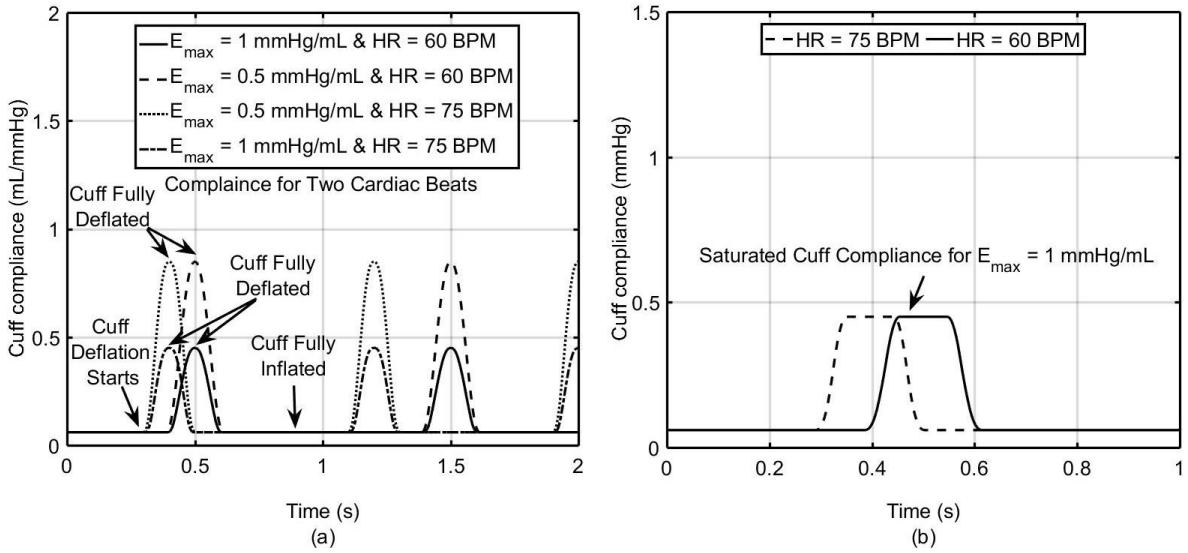

Figure 13. Extra-aortic cuff compliance profiles to inflate and deflate the proximal compartment (cuff) (a) shows the time varying cuff compliance at a HR of 60 and 75 BPM for LV elastance of 0.50 and 1 mmHg/mL, respectively (b) To limit the cuff volume to 30 mL the cuff compliance is restricted to 0.45 mL/mmHg for mild LV pressures (LV elastance of 1 mmHg/mL).

3.2.5.1. Cuff Compliance Deflation and Inflation Timing Optimization for single- and two-segmented CPDs

To optimize CO, the steepest descent technique was used to select deflation and inflation timing landmarks for the single- and two-segmented CPDs. Initially, the range of deflation and inflation times of the cuff compliance were referenced to the onset of AOF. The timing landmarks for cuff compliance deflation varied from 0.10 to 0.44 seconds, and inflation from 0.45 to 0.80 seconds. The rationale for choosing these ranges is to ensure the cuff compliance starts to increase at the opening of the aortic valve, and once the cuff is filled with 30 mL of blood volume, the compliance remains constant and then decreases, thereby optimizing KE. Initially, the area of AOF or stroke volume (SV) over a period of one beat was calculated between the deflation time of 0.40 seconds and inflation time of 0.70 seconds. A time shift (e.g. .0025 sec) was introduced to the deflation time of cuff compliance and the SV re-calculated to determine if the time shift resulted in an increased SV. The derivative calculated from the time shifts are given by:

$$\mathrm{d1} = \frac{\mathrm{area2} - \mathrm{area1}}{\mathrm{shift}}$$
$$\mathrm{d2} = \frac{\mathrm{area3} - \mathrm{area1}}{\mathrm{shift}} \tag{9}$$

where ‘shift’ is a small value of time (rate of change), ‘area1’ corresponds to the SV over a period of one cardiac cycle calculated on the initial points, ‘area2’ corresponds to the SV calculated after introducing small time shift in deflation time. Likewise, ‘area3’ corresponds to the SV calculated by shifting the inflation time with small time. In Equation (9), ‘d1’ is the search direction of deflation time and ‘d2’ is the search direction of inflation time to find the global maxima. Normalization of the derivatives was performed to make the directional vectors unity. Next, a new step size was calculated for deflation and inflation times to start moving in the direction of ‘d1’ and ‘d2’ (Equation (10)).

$$\mathrm{d1} > 0 \tag{10}$$
$$\mathrm{stepsize} = (\mathrm{T1max} - \mathrm{T1})/\mathrm{d1}$$
$$\mathrm{d1} < 0$$
$$\mathrm{stepsize} = (\mathrm{T1} - \mathrm{T1min})/\mathrm{d1}$$
$$\mathrm{d2} > 0$$
$$\mathrm{stepsize} = (\mathrm{T2max} - \mathrm{T2})/\mathrm{d2}$$
$$\mathrm{d2} < 0$$
$$\mathrm{stepsize} = (\mathrm{T2} - \mathrm{T2min})/\mathrm{d2}$$
$$\mathrm{stepsize} = \min(\mathrm{abs}(\mathrm{stepsize}))$$

where ‘T1max’ is the maximum value of the deflation time and ‘T1’ is the initial value of deflation time used to start the optimization process. Similarly, ‘T2max’ is the maximum value of inflation

time and ‘T2’ is the initial value of inflation time. The step size was divided into eight linearly spaced points and SV was calculated as shown in (Figure 14) to determine step size interval that results in maximum SV. The golden section method reduces the search space of step size interval. The step size interval with maximum SV further divided into two more points. In (Equation (11)) ‘f1’ and ‘f2’ are the functions used to generate two new step sizes between ‘a’ and ‘d’, the step size interval range. The SV was calculated for all four step sizes ‘a’, ‘b’, ‘c’, ‘d’, and these points were updated until the condition $\left(\mathrm{abs}(\mathrm{d}-\mathrm{a})\right) > 1\mathrm{e}^{-3}$ was satisfied.

$$\mathrm{f1} = \frac{3-\mathrm{sqrt}(5)}{2} \tag{11}$$

$$\mathrm{f2} = \frac{(\mathrm{sqrt}(5)-1)}{2}$$

$$\mathrm{a} = \mathrm{a0}$$

$$\mathrm{b} = \mathrm{a0} + \mathrm{f1}(\mathrm{d0}-\mathrm{a0})$$

$$\mathrm{c} = \mathrm{a0} + \mathrm{f2}(\mathrm{d0}-\mathrm{a0})$$

$$\mathrm{d} = \mathrm{d0}$$

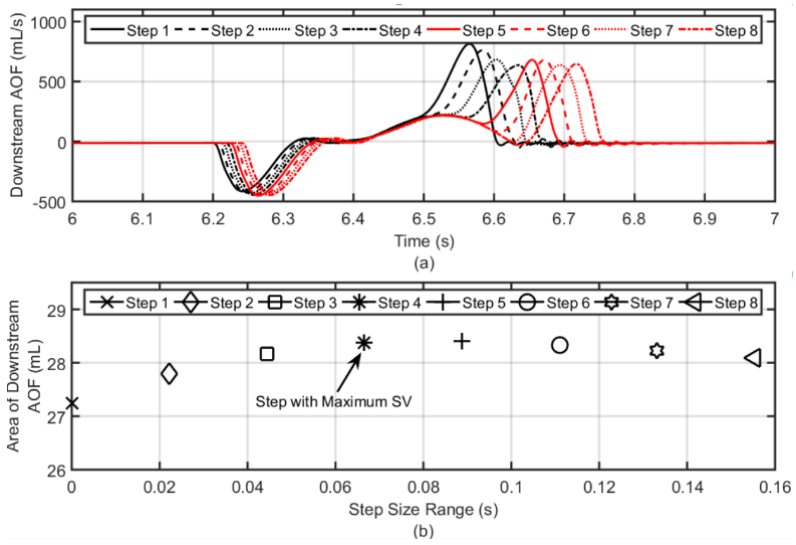

Figure 14. Optimization process of single cuff deflation and deflation timings (a) shows downstream AOF waveforms and (b) shows the corresponding SV at HR of 60 BPM and LV elastance (E_{max} = 0.50 mmHg/mL) for eight different deflation and inflation triggering times.

Finally, the optimal step size ‘P’ was chosen to correspond to maximum SV. The update equation of deflation ‘T1’ and inflation ‘T2’ time (Equation (12)) is iteratively adjusted until the difference between the updated and previous deflation and inflation times are greater than $1e^{-4}$.

$$\begin{aligned} T1 &= T1 + P * d1 \\ T2 &= T2 + P * d2 \end{aligned} \tag{12}$$

3.2.6. Concept of Optimizing Kinetic Energy

The experimental evidence established in [88] supports the idea that the LV actively draws the blood from left atrium (LA) during early diastole as the LV compliance is still increasing. Importantly, in terms of the flow’s driving energy expenditure, diastolic suction contributes to filling more than one order of magnitude above passive atrial decompression. The analysis has shown that diastolic suction in humans is initiated during isovolumic ventricular relaxation and continues during rapid filling. The diastolic nature of the LV has been well established in literature and we see that the variable compliance of the proximal compartment acting as a similar kind of suction (increasing compliance while filling).

To address the issues of modest increases in CO and retrograde flow associated with current MCSDs such as extra-aortic CPDs, we propose the development of an extra-aortic two-segmented CPD (Figure 15) designed to the idea of systolic suction and provide greater improvements in CO by harnessing the kinetic energy (KE) available in the forward aortic flow (AOF). The concept of optimizing the KE of forward AOF is taken from Bernoulli’s principle which says that total energy in a steady, frictionless, flow stream is the static pressure + the kinetic energy + the energy due to gravity. The actual AOF is neither steady nor frictionless, but Bernoulli’s equation shows, in a relatively straightforward way, how the various energies in a flow can be inter-converted for illustrative purposes.

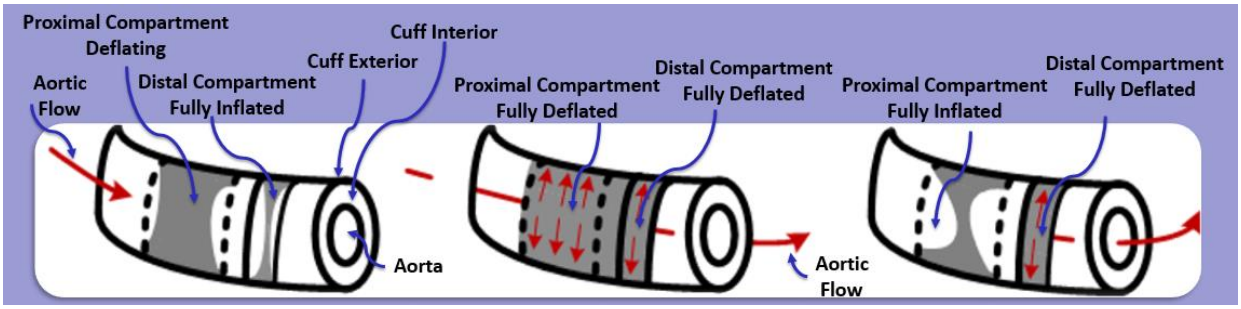

(a) (b) (c)

Figure 15. Side view illustration of extra-aortic two-segmented cuff consisting of proximal and distal compartments (a) represents the deflation of proximal compartment while the distal compartment remains fully inflated unless the proximal compartment is filled with 30 mL blood volume (during early systole), (b) shows proximal and distal compartments are fully deflated (during systole) and (c) shows proximal compartment is fully inflated and distal compartment is in deflation mode (during diastole). Timing of the cuffs are optimized to maximize the forward moving AOF and KE.

Simulations of cardiovascular system (CVS) assisted with extra-aortic single cuff CPD were carried out to determine the maximum dynamic pressure (or KE) presence in forward moving AOF. PV-Loops were generated for an assisted cardiac beat and maximum available dynamic pressure was added to it during the ejection phase. As shown in Figure 16 the difference between the total and static pressure in PV-Loop which is the dynamic pressure or KE ($1/2\ mv^2$) present in forward AOF during ejection. Total pressure of blood in vessel constitutes of static + dynamic pressure. An increase in the external work of LV can be achieved by optimizing the dynamic pressure or KE of forward AOF. In other words, the resulting dynamic pressure or KE yields a significant increase in CO. Table 5 lists several different scenarios for HR of 60 and 75 BPM with LV elastance of 0.50 to 1 mmHg/mL where a small percentage increase in the external work of LV due to dynamic pressure or KE in forward AOF produces a rise in CO.

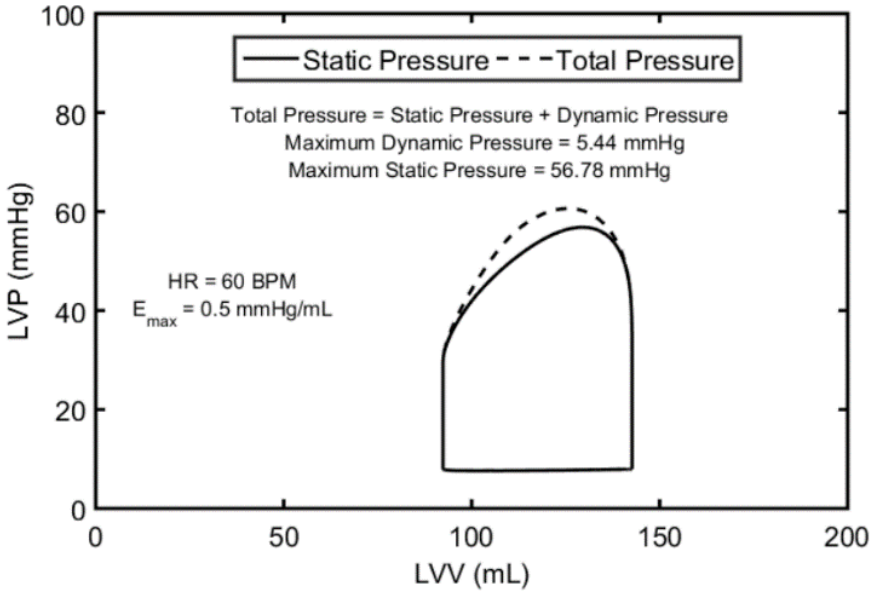

Figure 16. Demonstration of increase in external work of the LV, the difference between the total and static pressure is the dynamic pressure which represents the amount of KE energy that is available for optimization.

Table 5. Effect of left ventricle external work increase on cardiac output.

HR (BPM)	LV End-Systolic Elastance (mmHg/mL)	Maximum Dynamic Pressure (mmHg)	% Increase in ELVW	Increase in CO (L/min)
60	0.50	5.44	2.36	0.55
	0.75	7.64	2.57	0.35
	1.00	9.48	2.72	0.23
75	0.50	6.06	2.94	0.93
	0.75	9.07	3.59	0.88
	1.00	11.18	3.30	0.50

In concept, a large proximal CPD compartment will fill with forward-moving AOF, and an inflated distal CPD compartment will act as a control valve to prevent backflow from the aorta downstream of the CPD. Any retrograde flow will reduce proximal compartment volume capacity while also reducing forward AOF KE. Once the proximal compartment has been filled, the distal CPD compartment will open in a manner to optimize the forward AOF KE, thereby increasing the effectiveness of the assist device. In this paper, we present the optimization of KE to increase

device effectiveness and show, by way of an example, the hemodynamic and LV pressure–volume responses to extra-aortic single and two-segmented CPD for sever and mild HF cases.

3.2.7. Modeling the Extra-Aortic Two-Segmented Cuff CPD

The extra-aortic two-segmented CPD was modeled using an electrical switch to represent the distal compartment, with the opening and closing of this switch regulated by an external controller (Figure 17). During LV systole, the proximal compartment was filled with upstream AOF with the switch open (modeled as small compliance), such that there is no downstream retrograde flow back-filling the proximal compartment of the CPD. When the proximal CPD compartment reached both its maximum compliance and was filled with 30 mL of blood volume, the distal compartment deflates (switch closes), which results in minimum backflow of downstream AOF into the proximal compartment volume. The opening of the switch and the subsequent filling of an extra-aortic cuff with upstream flow helps to maintain KE moving from the LV to the aorta.

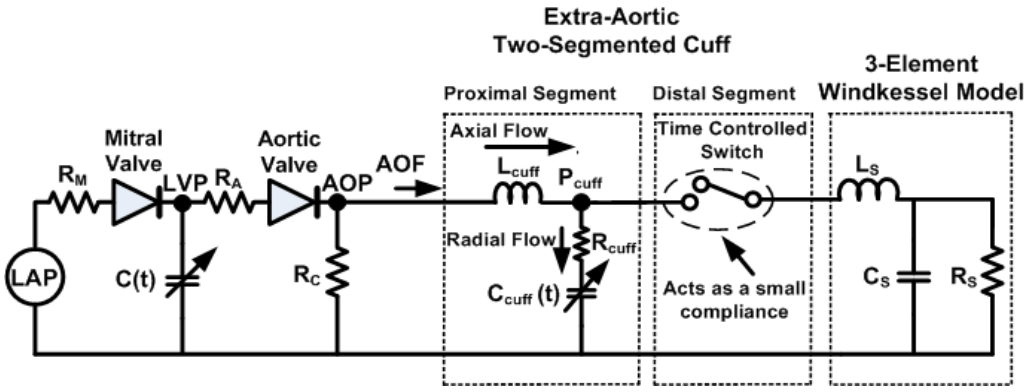

Figure 17. Integration of the CVS model with the extra-aortic two-segmented cuff CPD consisting of: 1) proximal segment and 2) distal segment.

3.3. Results

Simulated hemodynamic waveforms and LV PV-loop for the severe HF test condition (60 BPM HR, 3 cardiac beats, 7-10 sec) are shown in Figure 18. The simulated waveform data

produced clinically equivalent responses for a decrease in LV elastance from 2 mmHg/mL (normal, healthy) to 0.50 mmHg/mL (HF). Specifically, reductions in LV diastolic (33 mmHg) and systolic (51 mmHg) pressures, CO (1.85 L/min), LVEF (22%), diastolic CAF (3 mL/s), MAP (38.7 mmHg) and peak LVP systolic (52.1 mmHg) were predicted.

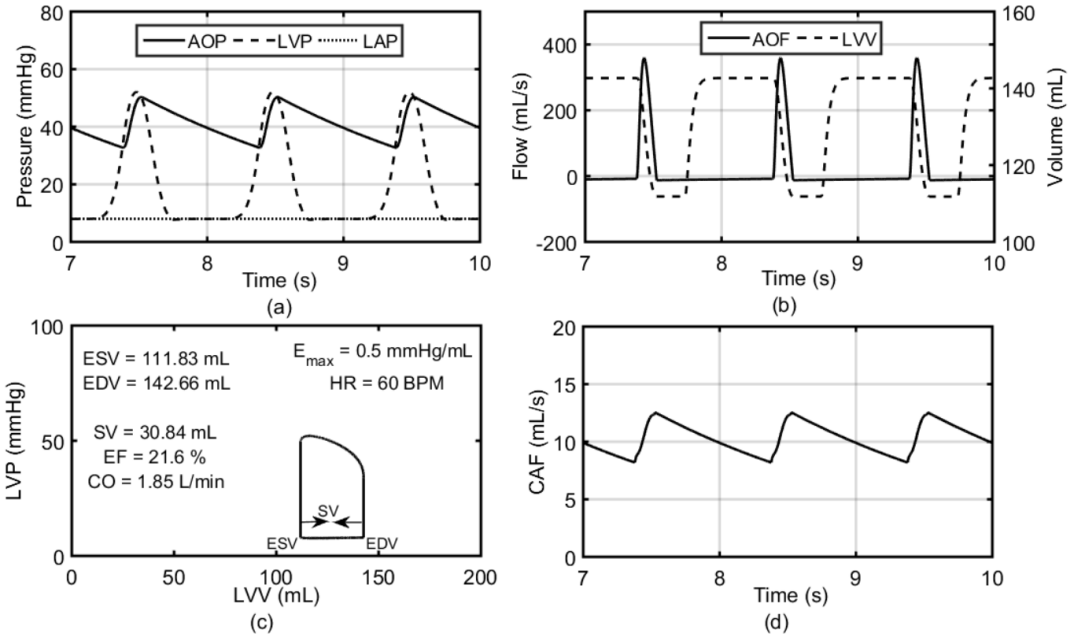

Figure 18. Severe HF test condition at HR of 60 BPM (a) shows the pressure waveform of aorta, LV and LA (b) shows the AOF and LVV (c) shows the PV-loop of LV and (d) shows the diastolic CAF and the augmentation in flow during systole.

The extra-aortic single cuff CPD simulation during the severe HF test condition predicted a maximum compliance of 0.85 mL/mmHg is required to displace 30 mL of volume per beat into the cuff to reduce LV workload, increase diastolic CAF, and increase the CO (Figure 19). The pressure waveforms demonstrate the potential for diastolic augmentation (increases of 24-69 mmHg) and 10 mmHg increase in peak LV systolic pressure. Similarly, the flow waveforms predict increases in downstream AOF and LVV, 2 mL/s increase in diastolic CAF, and 33% improvement in LVEF. The PV-loop data suggest a 33% improvement in CO with the single-cuff CPD.

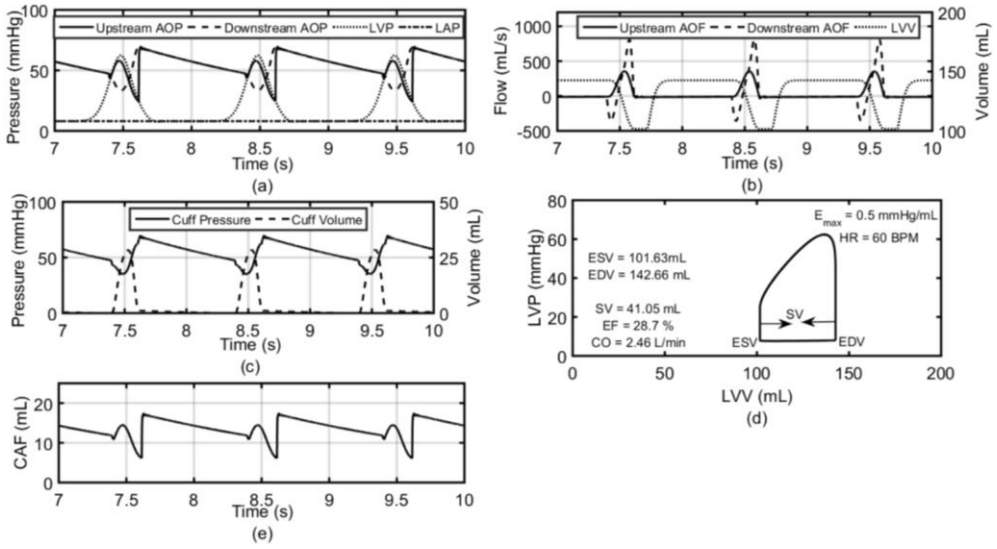

Figure 19. Extra-aortic single cuff CPD for severe HF at HR of 60 BPM (a) shows the pressure waveforms of upstream and downstream aorta, LV and left atrium (b) shows the upstream and downstream AOF (retrograde flow can be seen) and LVV (c) shows the pressure and volume in cuff (d) shows the PV-loop of the LV and (e) shows the diastolic CAF and the augmentation in the flow during systole.

The predicted hemodynamic and LV PV-loop data for the extra-aortic two-segmented cuff CPD during severe HF model test condition are shown in Figure 20. Importantly, the flow waveforms demonstrate that the two-segment cuff minimizes the reverse flow that was observed with single-cuff CPD. Oscillations in the hemodynamic waveforms with the two-segmented CPD were likely due to the abrupt opening and closing of the switch, which was used to model the behavior of the distal CPD segment. The additional increase in AOF supports the concept of optimizing forward KE transfer. The pressure waveforms also predict an additional increase in diastolic augmentation (30 to 89 mmHg) with a reduction in peak LVP systolic (56 mmHg). The flow data also suggest additional increases in diastolic CAF (8 mL/s) and LVEF (35%), and CO (3.0 L/min, 23% improvement) compared to the single-cuff CPD. Computer simulations with single-cuff and two-cuff CPD were repeated during mild HF (Figure 21), which also showed improvements in cardiac function as shown in single-cuff (Figure 22) and two-cuff (Figure 23) respectively.

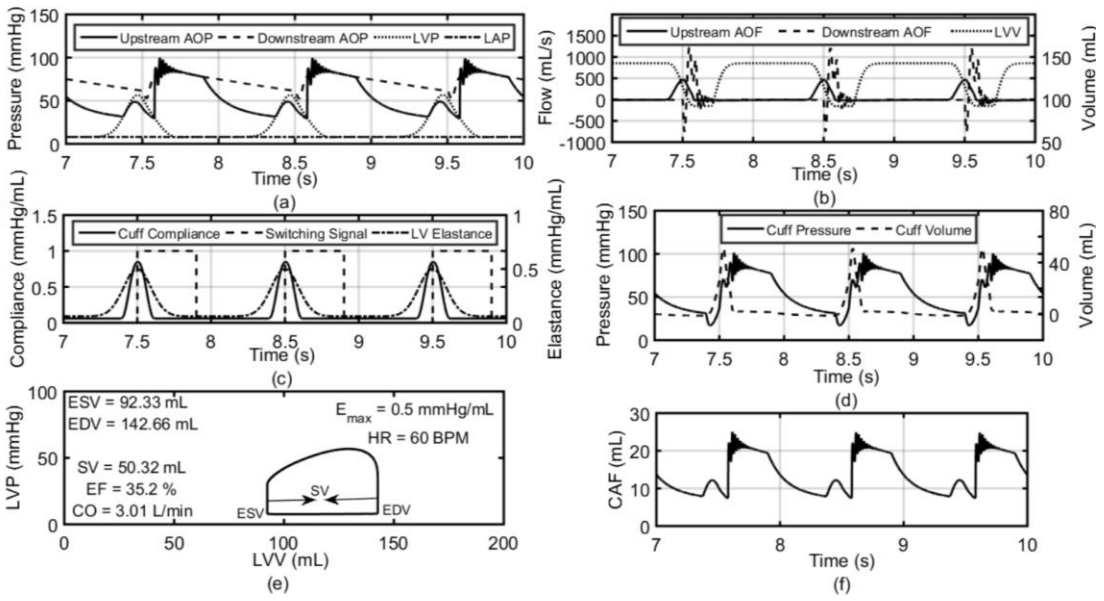

Figure 20. Extra-aortic two-segmented cuff CPD for severe HF at HR of 60 BPM (a) shows the pressure waveforms of upstream and downstream aorta, LV and left atrium (b) shows the upstream and downstream AOF (retrograde flow is minimized) and LVV (c) shows the cuff compliance of proximal segment, the switching signal waveform indicates the opening and closing of distal segment and the LV elastance (d) shows the pressure and volume in cuff (e) shows the PV-loop of the LV and (f) shows the diastolic CAF and the augmentation in the flow during systole.

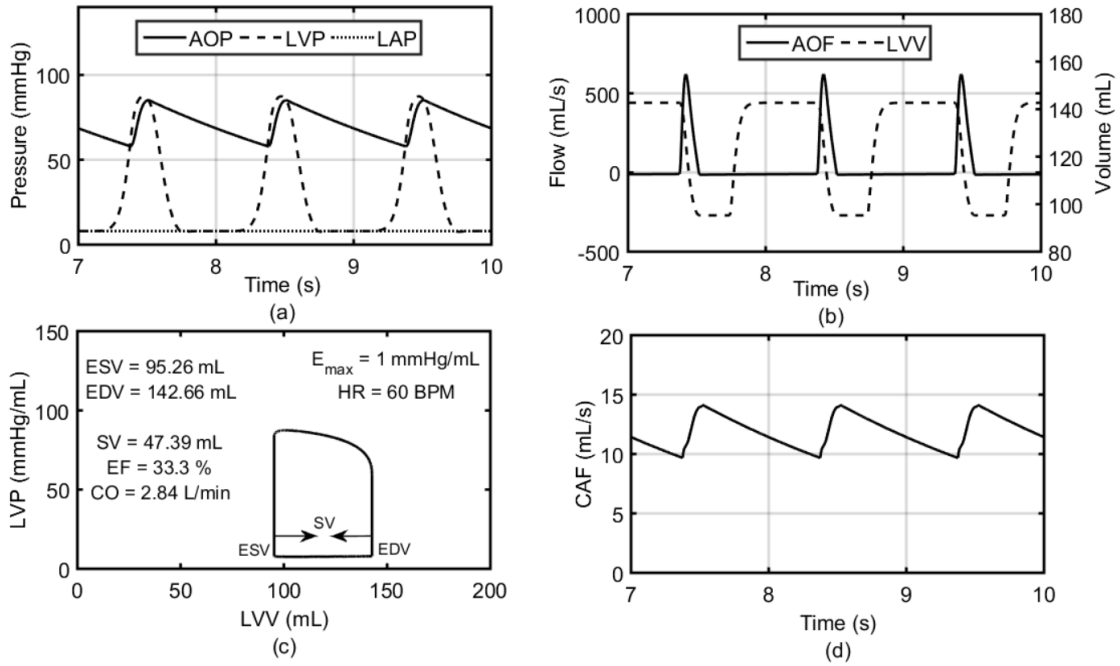

Figure 21. Mild HF test condition at HR of 60 BPM (a) shows the pressure waveform of aorta, LV and LA (b) shows the AOF and LVV (c) shows the PV-loop of LV and (d) shows the diastolic CAF and the augmentation in flow during systole.

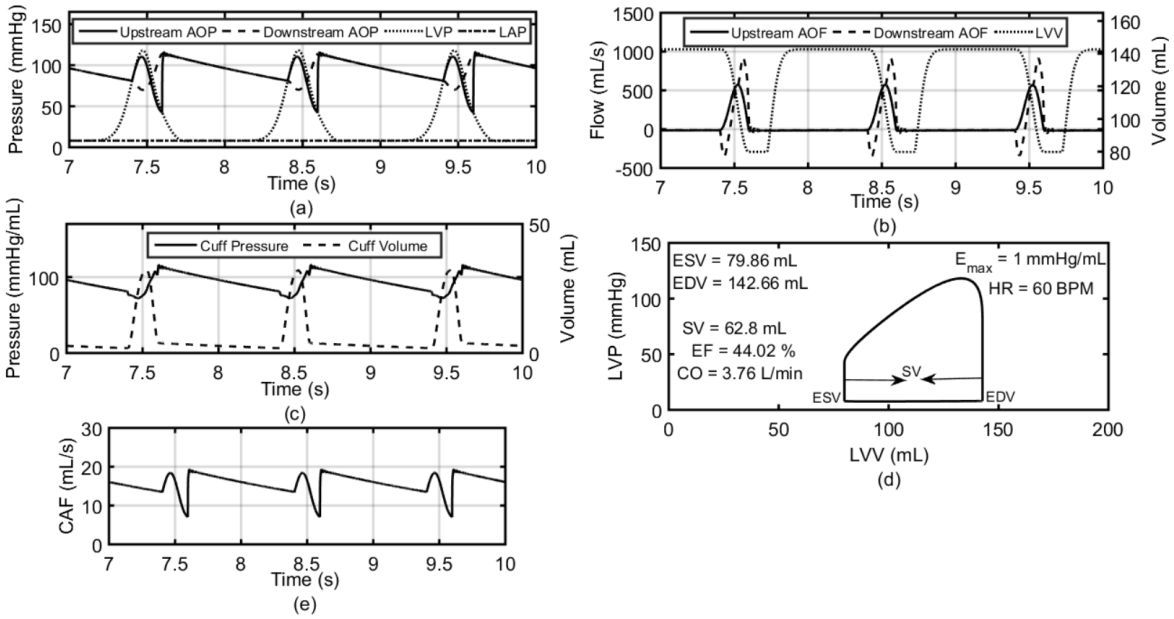

Figure 22. Extra-aortic single cuff CPD for mild HF at HR of 60 BPM (a) shows the pressure waveforms of upstream and downstream aorta, LV and left atrium (b) shows the upstream and downstream aortic flow (retrograde flow can be seen) and LVV (c) shows the pressure and volume in cuff (d) shows the PV-loop of the LV and (e) shows the diastolic CAF and the augmentation in the flow during systole.

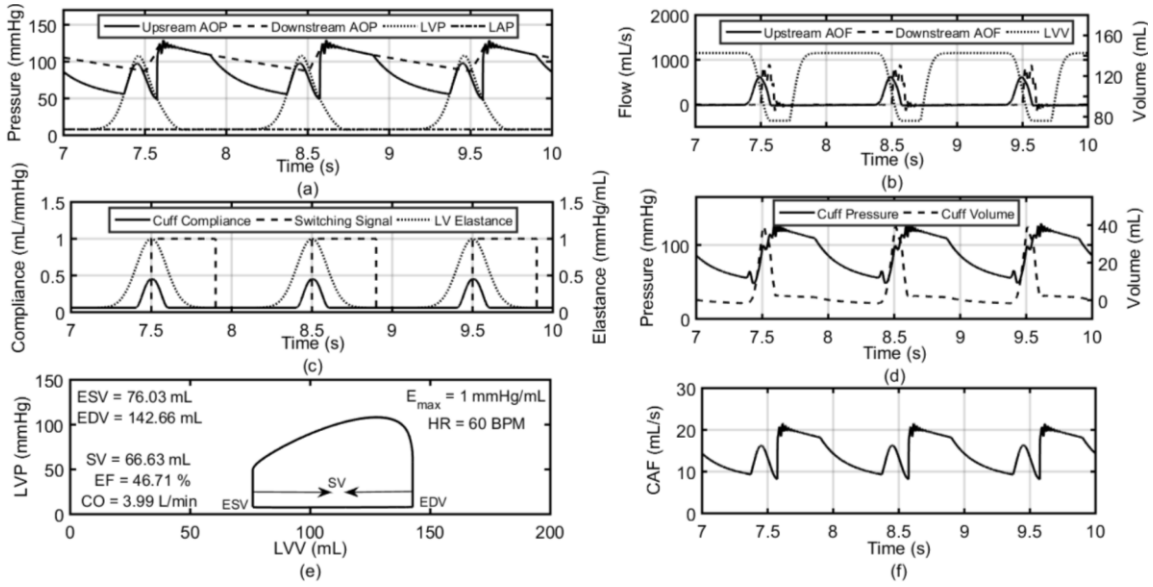

Figure 23. Extra-aortic two-segmented cuff CPD for mild HF at HR of 60 BPM (a) shows the pressure waveforms of upstream and downstream aorta, LV and LA (b) shows the upstream and downstream AOF (retrograde flow is minimized) and LVV (c) shows the cuff compliance of the proximal segment, the switching signal waveform indicates the opening and closing of distal segment and LV elastance (d) shows the pressure and volume in cuff (e) shows the PV-loop of the LV and (f) shows the diastolic CAF and the augmentation in the flow during systole.

Computer simulations were then repeated for HR of 75 and 120 BPM with E_{max} of 0.50 and 1 mmHg/mL respectively have also shown improvement in cardiac function (Figure 24). The hemodynamic responses to single and two-segmented CPD for HR of 60 and 75 BPM with E_{max} of 0.50 mmHg/mL are shown in Figure 25, demonstrating that the two-segmented CPD increased the AOF velocity, optimized the KE of AOF to increase SV and CO, and minimized the retrograde AOF.

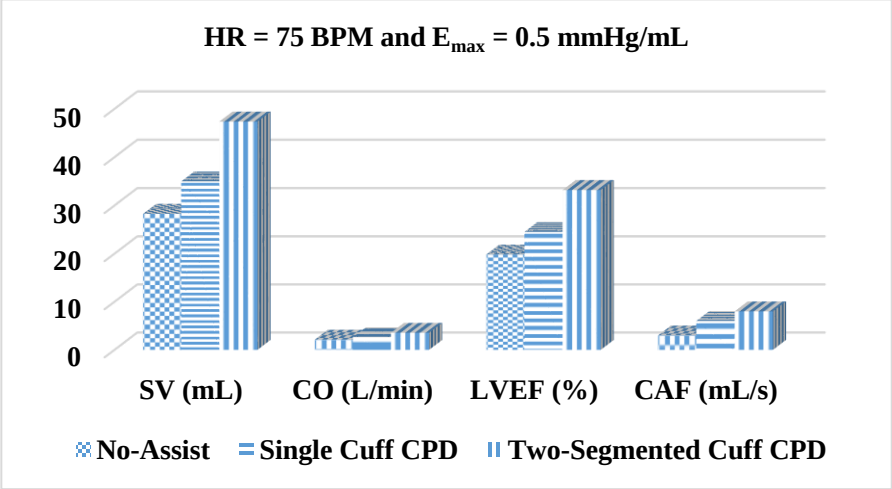

(a)

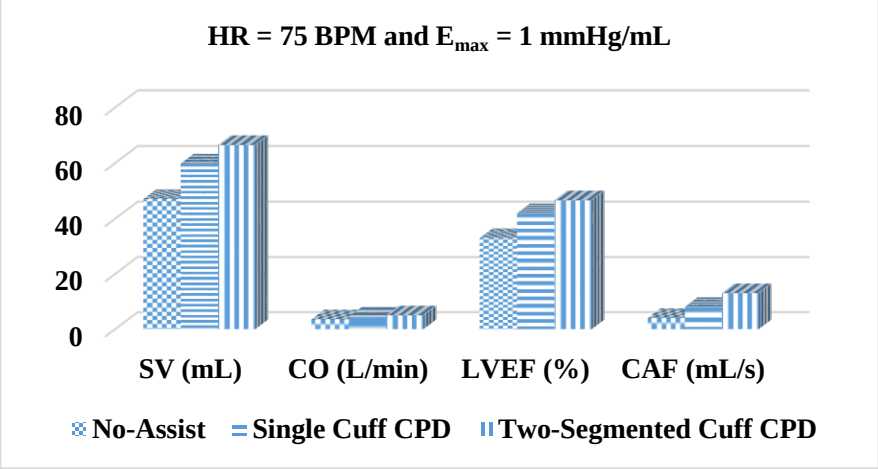

(b)

Figure 24. Shows the comparison of SV, CO, LVEF and CAF for no-assist, single cuff and two-segmented cuff CPD at HR of 75 and 120 for LV elastance of 0.5 and 1 mmHg/mL representing severe and mild HF.

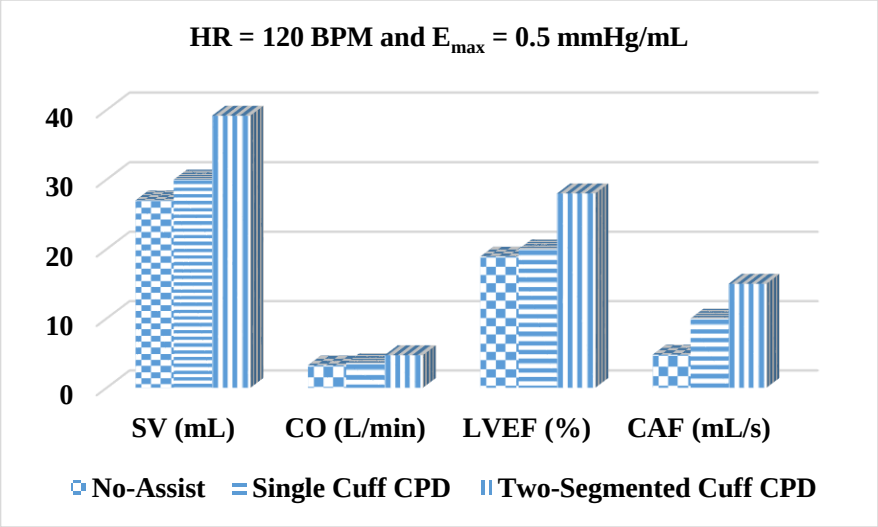

(c)

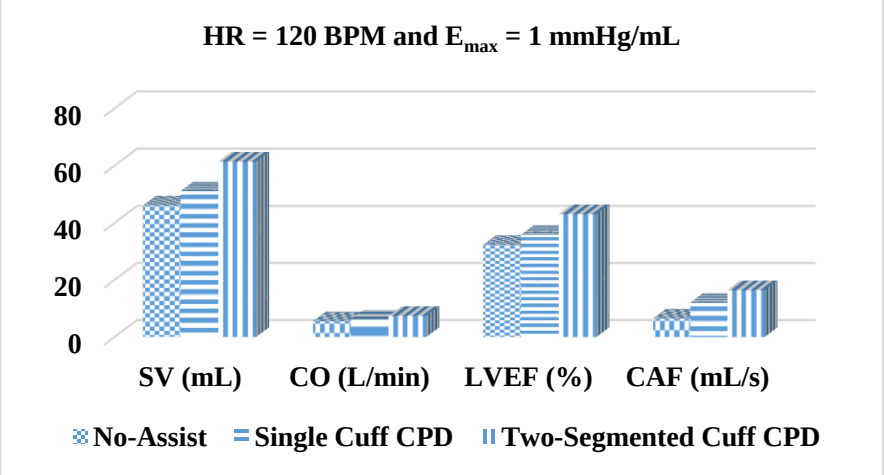

(d)

Figure 24. Shows the comparison of SV, CO, LVEF and CAF for no-assist, single cuff and two-segmented cuff CPD at HR of 75 and 120 for LV elastance of 0.5 and 1 mmHg/mL representing severe and mild HF (continued).

For sensitivity analysis of the reported results ±10% uniform variations were introduced in the CVS arterial parameters and simulations were performed for no-assist and with device (single cuff and two-segmented cuff) assistance. Figure 26. Sensitivity analysis of CVS Simulink HF model with no-assist, single cuff and two-segmented cuff assist models. The top three plots in

figure shows the variation in parameters of arterial compliance, resistance and inductance at HR of 60 BPM at LV elastance of 0.5 mmHg/mL (severe HF). Similarly, bottom three plots are for LV elastance of 1 mmHg/mL (mild HF). The dotted line in plot shows the CO for tuned CVS HF model (no-assist) with no parameter variation. Figure 26 shows the plots of variation in arterial compliance (C_S), arterial resistance (R_S) and arterial inductance (L_S) of the no-assist, single cuff and two-segmented cuff system at a HR of 60 BPM and LV elastance of 0.5 and 1 mmHg/mL respectively. Similar responses were achieved for the sensitivity analysis of 75 and 120 BPM. During each sensitivity analysis one arterial parameter was varied at a HR of 60, 75 and 120 BPM for LV elastance of 0.5 to 1 mmHg/mL.

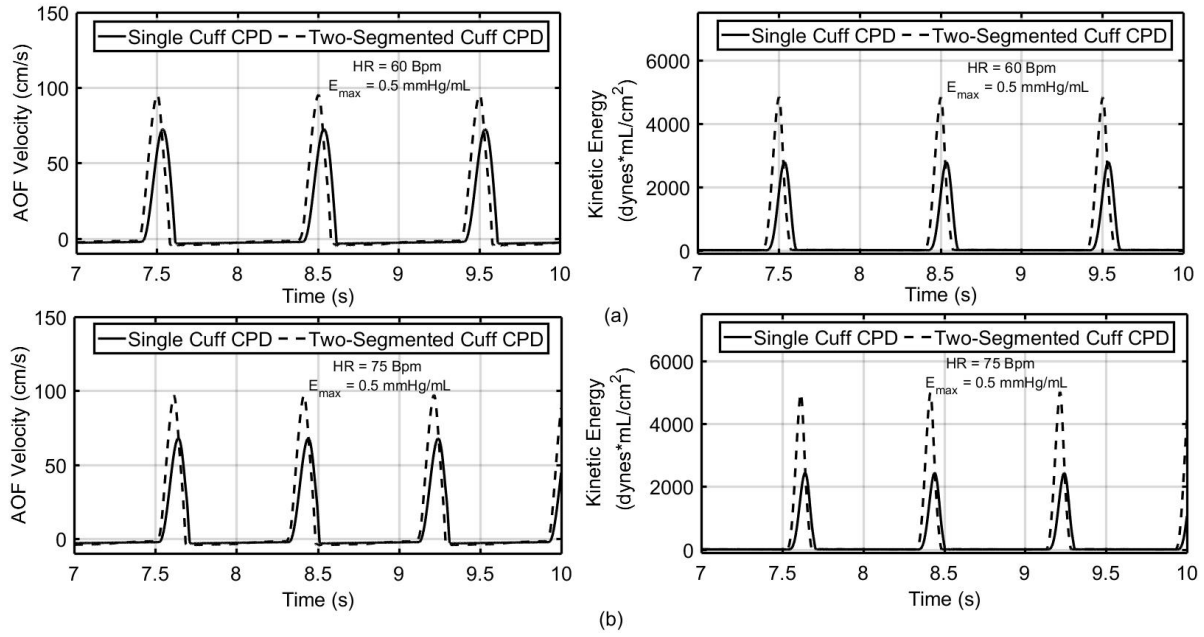

Figure 25. Increase in AOF velocity and enhancement of forward KE (a) and (b) show the AOF velocity and corresponding KE increase using extra-aortic two-segmented CPD over a period of three cardiac beats at HR of 60 and 75 BPM for LV elastance of 0.50 mmHg/mL.

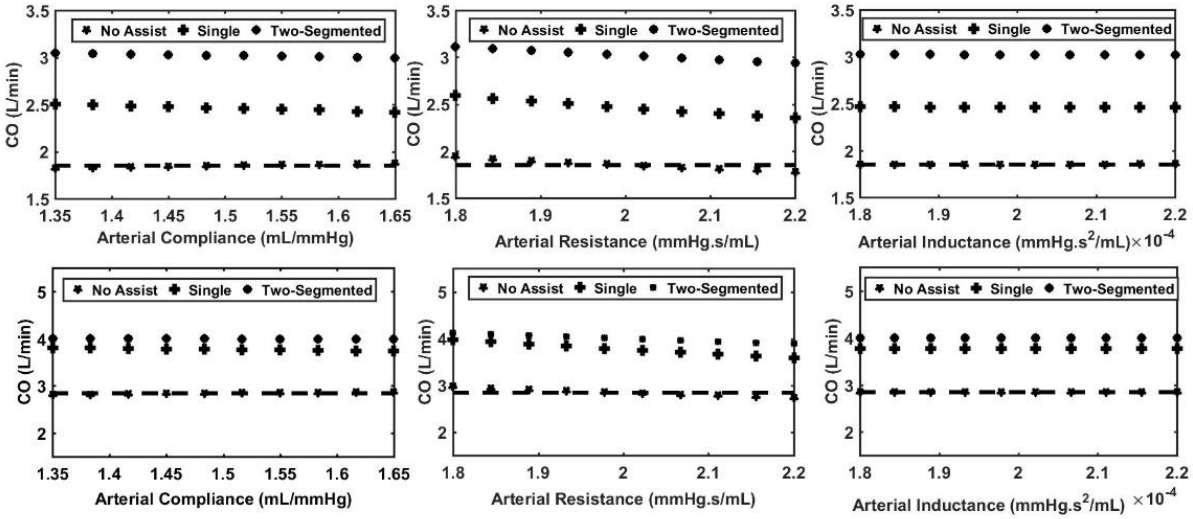

Figure 26. Sensitivity analysis of CVS Simulink HF model with no-assist, single cuff and two-segmented cuff assist models. The top three plots in figure shows the variation in parameters of arterial compliance, resistance and inductance at HR of 60 BPM at LV elastance of 0.5 mmHg/mL (severe HF). Similarly, bottom three plots are for LV elastance of 1 mmHg/mL (mild HF). The dotted line in plot shows the CO for tuned CVS HF model (no-assist) with no parameter variation.

3.4. Discussion

Some patients with moderate to severe HF require advanced therapy once optimal medical (OMM) and (CRT) are no longer effective. Once the safety, reliability, and efficacy of MCSDs has been demonstrated and clinically accepted, their utility may expand to class III and ambulatory class IV HF patients [40]. CPDs, such as IABP, can only provide short-term, modest improvements in cardiac function, blood contacting with added risk of adverse events, restrict patient mobility, and at risk for limb ischemia. MSCDs with extra-aortic CPD are non-blood contacting and may provide better hemodynamic advantages, enable patient mobility, and offer long-term ambulatory use [69]. Giridharan et al. reported that two counterpulsation devices, one that wraps around the aorta and the other that is anastomosed to the aorta, provided hemodynamic improvements comparable to IABP [73]. During the rapid deflation of a MCSDs e.g. IABP/extra-aortic CPD,

aortic end-diastolic pressure drops rapidly producing a "steal" phenomena (retrograde blood flow), which limits the amount of diastolic CAF and CO augmentation [89].

Sensitivity analysis of the reported results suggest that an increase in arterial compliance and inductance of the CVS model (no-assist) slightly increased the CO whereas increases in arterial resistance decreased the CO, independent of HR and LV elastance. However, for the case where the CVS model is integrated with single and two-segmented models (assisted), increase in arterial compliance and inductance reduced the CO and the variation in arterial resistance behaved the same as in case of no-assist. In summary of the sensitivity analysis we concluded that ±10% uniform variation in arterial parameters of the CVS model has a minimum effect on the system performance and CO.

In a study conducted by Schulz *et al.*, C-Pulse system was implanted for 6 months in 8 patients, 4 of which had ischemic and 4 had non-ischemic cardiomyopathy and preliminary site reported data was presented. No device related injury like stoke, myocardial infraction, major bleeding or major infection were reported. Within 6 months of observation the functional status of patients enhanced from NYHA class III to II for 5 patients while 2 remained in class III. It is also reported in this study that with C-Pulse system the mean LVEF for NYHA class III patients improved from 24±8% to 45±5% [90] which is comparable to our reported results. In our simulation, the baseline (no-assist) LVEF (35%) for mild HF patient (class III) increased with single (45%) and two-segmented (49%) CPDs.

KE of blood in the aorta is given by the relationship $(1/2\rho v^2)$, where ρ is the density and v is the velocity of blood flow. Tortora *et.al.* reported that the total cross sectional area of human aorta normally varies between 3 to 5 cm^2 and has a velocity of 40 cm/s [91]. David et al. reported that in mammals the maximum blood velocity occurs at the base of aorta at a peak of ventricular

ejection and is about 50 cm/s [92]. He also reported that the KE of blood in aorta during peak ejection is 1319 dynes*mL/cm^2 (without any assist device). In our simulation results, the velocity of AOF is given by the relationship $velocity = (AOF/Area)$. The AOF at the peak of ventricular ejection was found to be 378 mL/s for severe HF at HR of 60 BPM using single cuff and 468 mL/s using two-segmented cuff CPD for a cross sectional area of 4.91 cm^2. The peak AOFs found are relatively high for heart in failure, however the average SV is well under normal limit and this is mainly due to the LV elastance narrow ejection period. The velocity of AOF was calculated to be 76 cm/s and 96 cm/s for single and two-segmented cuff CPDs. The higher AOF velocity (+20 cm/s) with the two-segmented CPD generates greater KE. Specifically, the KE of forward moving AOF at a blood density of 1.06 gm/cm^3 during peak ejection was calculated to be 3061 dynes*mL/cm^2 for single and 4834 dynes*mL/cm^2 for two-segmented CPD.

In a study conducted by Schulz et al., C-Pulse system was implanted for 6 months in 8 patients 4 of which had ischemic and 4 had non-ischemic cardiomyopathy and preliminary site reported data was presented. No device related injury like stoke, myocardial infraction, major bleeding or major infection were reported. Within 6 months of observation the functional status of patients enhanced from NYHA class III to II for 5 patients while 2 remained in class III. It is also reported in this study that with C-Pulse system the mean LVEF for NYHA class III patients improved from 24±8% to 45±5% [90] which is comparable to our reported results. In our simulation, the baseline (no device) LVEF (35%) for mild HF patient (class III) increased with single (45%) and two-segmented (49%) CPDs.

The predicted hemodynamic responses represent a significant improvement compared to Legget et al [73]. During 1:1 counterpulsation the peak diastolic augmentation pressure was found to be 111 mmHg and 127 mmHg for extra-aortic single and two-segmented CPDs, respectively

compared to 94 mmHg reported by Legget et al. Also, a two-segmented CPD may prevent retrograde flow by using a distal compartment of the CPD as a valve until the filling of the proximal compartment cuff occurs. Moreover, there is evidence that CP is more effective when performed with a counterpulsation sac (volume displacement) than with an IABP (pressure displacement) of the same or larger size [9].

Many clinical studies have been performed to assess the effect of extra-aortic CPD aortic wall structure. Cheng et al. examined the histological and clinical data of patient supported on C-Pulse for a period 21 months [93]. One month after implantation patient symptoms improved from NYHA class III to class I, and the CO increased from 3.5 to 5.5 L/min, which is comparable to the simulation results predicted in our study. Specifically, for LV elastance of 1 mmHg/ml at HR of 75 BPM, and baseline CO of 3.7 L/min, the CO increased to 4.8 L/min with extra-aortic single CPD and 5.2 L/min with extra-aortic two-segmented CPD. Cheng et al. also showed that extra-aortic CPDs do not appear to alter aortic wall structures [93]. In conclusion, the results of this study demonstrate that the concept of KE optimization may enhance the CO of assist devices such as an extra-aortic CPD that reduces backflow and times the forward KE.

3.5. Limitations

The simulation model relies on a number of simplifying assumptions that may impact our study results; however, this work provides an initial step in device development and evaluation of control algorithms. For example, the computer model assumes ideal valves that open and close instantaneously, Newtonian fluid, and does not account for inertial or gravitational effects. Also, only the left heart was programmed to be dysfunctional in this model with the right heart programmed with normal function. As the simulation model relies on number of simplifying assumptions, this limits the capability of the model. In this computational study, a switch was used

to represent the inflation and deflation of the distal compartment. Certainly, the HF model is a simplification of complex dynamics. However, the primary value of the computer simulation was the development of the timing algorithm and device control strategies and demonstration of proof-of-concept. Future work is to assess the best device for implementation of the KE concept (or the types of devices that may benefit from optimizing KE) followed by a bench-top demonstration and finally an animal model verification.

4. OPTIMAL TIMING CONTROL OF EXTRA-AORTIC TWO-SEGMENTED COUNTERPULSATION DEVICE BY EXHAUSTIVE SEARCH

This paper will be submitted to Cardiovascular Engineering and Technology journal. This chapter discusses the exhaustive search technique to find out the best compliance profile and the increase in CO achieved through this optimized timing cuff compliance profile as compared to the optimization performed previously with steepest decent and golden section method. This chapter also discusses the four different timing modes of cuff compliance inflation and deflation, and statistically compares the significant difference in hemodynamic parameters of no-assist device with four timing modes of two-segmented CPD.

4.1. Introduction

HF is the most common diagnosis of hospital admission in patients above 65 years in high-income countries. The incidence of CHF is increasing worldwide, with more than 1 million admissions diagnosed annually in the United States and with the comparable percentage in Europe [90]. Even with well-managed therapies such as pharmacologic or CRT sometimes it is inadequate to ensure a satisfactory level of cardiac function for most patients with severe HF. Only cardiac transplantation offers the optimal treatment for long-term survival, however, it is limited by donor availability [9]. In some cases MCSDs are considered as a bridge to recovery for severe HF patients [94].

Counterpulsation therapy is the earliest form of MCSD and is widely used in the form of IABP for short-term treatments with up to 65% successful clinical results [68]. Counterpulsation provides important clinical benefits for the heart including diastolic augmentation with increased coronary perfusion and reduces the LV workload. However, the biocompatibility issues associated with IABP limits the application of an IABP to short periods (<14 days), for over (>20 days) the

rate of vascular complications were potentially greater [9], [90]. To overcome these limitations and utilize the proven benefit of counterpulsation therapy extra-aortic CPDs have been developed that are non-blood contacting, less invasive and don't require the patient to remain supine during the time of therapy unlike IABP [90].

Extra-aortic balloon (EAB) counterpulsation is a pneumatically driven balloon cuff that can be surgically positioned around the ascending aorta through a marginally invasive approach, consisting of a bipolar ECG lead, and a percutaneous driveline connecting the system to an external driver (Figure 6). The inflation and deflation of a balloon is ECG triggered. The deflation starts before the opening of aortic valve i.e. pre-R-wave deflation and continues during systole, whereas inflation starts after the closure of aortic valve i.e. post-dicrotic notch inflation. This therapy is recommended for patients with moderate to severe HF according to American college of cardiology/ American Heart Association (ACC/AHA), typically for stage C and NYHA functional class III or ambulatory class IV HF patients.

Improvements in diastolic CAF and reductions in LV afterload and external work has been well-documented in many short-term studies [73]. However, it has also been reported that MCSDs with EAB counterpulsation may produce retrograde flow during diastole that can reduce the CO and coronary flow to arteries. Overall, CPDs are considered insufficient to meet the needs of NYHA ambulatory class IV HF patients [10].

To address these issues with current MCSDs of modest increases in CO and retrograde flow associated such as EAB CPDs, Qureshi et al. proposed the development of an extra-aortic two-segmented CPD simulation model to provide greater improvements in CO by harnessing the KE available in the forward AOF [95]. This idea of optimizing KE of forward AOF was taken from Bernoulli's principle which says that total energy in a flow steam is the sum of static pressure,

KE and PE. Simulation results of PV-loop presented in this work strengthen the concept that even a few percent increment in dynamic pressure or KE yields a more significant increase in CO. The authors presented the optimization of KE to increase device effectiveness and showed, by way of an example, the hemodynamic and LV-PV responses to no-assist, extra-aortic single and two-segmented CPD for severe to the mild HF cases. However, this work didn't address the optimal timing of extra-aortic CPD (deflation and inflation) to provide optimal hemodynamic improvements. Therefore, we present the predicted hemodynamic and LV-PV response to severe to mild HF of extra-aortic two-segmented CPD using steepest descent and exhaustive search optimization techniques. We also compare the hemodynamic response for sick heart and with two-segmented CPD support for four control modes through a computer model of left heart of the cardiovascular system (CVS).

4.2. Materials and Methods

4.2.1. Overview of Two-Segmented Cuff Counterpulsation Device

The goal of counterpulsation therapy is to utilize mechanical device to augment the pressure during diastole to increase CAF by pushing the blood (inflation) and lowering the LV workload during systole by reducing the aortic pressure (AOP) (deflation). The two-segmented CPD works exactly on the same principles of single cuff CPD to achieve similar hemodynamic benefits. However, this device also optimizes the KE of the forward moving blood and minimizes retrograde flow which was a major impeding factor in achieving greater CO in previous extra-aortic CPDs. The extra-aorta two-segmented model consists of two compartments: (1) proximal and (2) distal. In concept, a large proximal compartment is filled with forward moving AOF during native heart systole (deflation), and an inflated distal compartment acts as a control valve to prevent backflow from the aorta downstream of the CPD. The proximal compartment starts ejecting

(inflation) once filled with required volume and distal compartment deflates during native heart diastole. Any retrograde flow will reduce proximal compartment volume capacity while also reducing the forward AOF KE. The objective here is to open distal compartment in a manner to optimize the forward AOF by maintaining the KE, thereby increasing the effectiveness of the assist device.

4.2.2. Computer Simulation Model

A thorough explanation of the computer simulation electrical equivalent model of the CVS used in this article has been previously provided (Qureshi et al., 2016) and used to develop and test physiologic responses of single and two-segmented CPD [95]. In this model, every chamber in the CVS is defined by its resistance (R) to the flow of blood and its compliance (C) that represents the ability to store blood volume (V). The right heart and pulmonary network parameter were assumed to mimic healthy state. In its simplest configuration, the model has one pressure source (left atrium pressure), two heart valves (mitral and aortic), and three blocks including LV, aorta, and coronary circulation. The proximal compartment of extra-aortic two-segmented CPD was modeled with three elements: (1) time-varying compliance ($C_{cuff(t)}$), (2) inductance (L_{cuff}) representation the inertia of blood, and (3) a small internal resistance to model the frictional losses and the distal compartment is modeled with the help of electrical switch to mimic the behavior of small cuff compliance.

In this model, the proximal compartment displaces up to 30 mL of blood volume per cardiac cycle [96]. The relationship of proximal compartment filling and ejection is given by the relationship $dV(t)/dt = Flow_{in} - Flow_{out}$, where $V(t)$ is the blood volume in the proximal compartment, $Flow_{in}$ is the flowrate into the proximal compartment during systole, $Flow_{out}$ the flow out of the proximal compartment during diastole. $Flow_{out}$ is zero during the systole when the

proximal compartment is being filled (30 mL) with forward moving AOF (deflation) and the distal compartment is fully inflated (switch open), to make sure that no downstream AOF going into the proximal compartment to minimize the retrograde flow and $Flow_{in}$ is zero during diastole when the proximal compartment (inflation) starts ejection and the distal compartment deflates (switch close). The opening of the switch and the subsequent filling of the proximal compartment with upstream flow helps to maintain KE moving from LV to the aorta. A wide range of HF scenarios was simulated ranging from mild to severe (Table 6) [83]. The level of HF is represented by the stiffness of the LV muscle [86] the patient's activity level by adjusting systemic resistance (R_s), and variations in the HR from 60 to 100 BPM.

Table 6. Heart failure scenarios for 60, 75, and 100 BPM [86].

HR (BPM)	Systemic Resistance (mmHg.s/mL)	Activity Level	E_{max} = 1.00 (mmHg/mL)	E_{max} = 0.75 (mmHg/mL)	E_{max} = 0.50 (mmHg/mL)
60	2.00	Inactive	Mild HF	Moderate HF	Severe HF
75	1.75	Active	Mild HF	Moderate HF	Severe HF
100	1.50	Very Active	Mild HF	Moderate HF	Severe HF

4.2.3. Optimal Timing Exhaustive Search

In this study 1:1 support mode (1 counterpulsation per cardiac cycle) was used. CPD filling and ejection morphology (bell-shaped) was generated using cubic spline interpolation. This method requires a minimum of three-time points to represent the process of deflation (increase in compliance of proximal compartment) and inflation (decrease in compliance of proximal compartment) of extra-aortic two-segmented CPD. Depending on the HR (Table 7) cardiac beat is divided into three time slots (Figure 27): (1) deflation start time (40% of the cardiac beat), (2) deflation end time and inflation start time (20% of the cardiac beat), and (3) inflation end time (40% of the cardiac beat). Seven linearly spaced time points are generated in each time slot and

each slot is further divided from the median point into two sub time slots *early* and *late* with three time points in each sub-slot. For three-time slots with seven time points in each slot a total of 343 unique combinations were obtained. Similarly, for each combination of three time points the cuff compliance profile was generated, and through exhaustive search timing relative to maximum CO was determined.

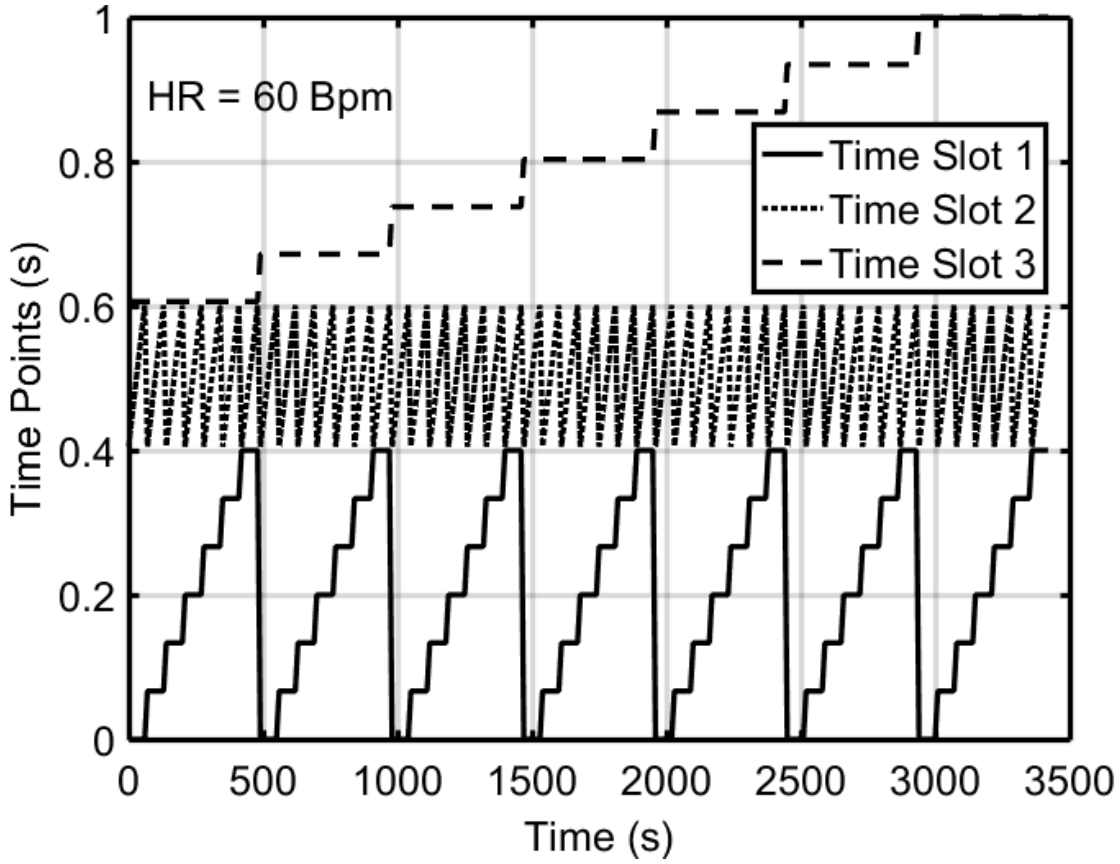

Figure 27. Various combinations of three-time slots to map out exhaustive search. These combinations of time slots were used to create compliance waveforms for inflation and deflation of proximal cuff (compartment).

For each profile, ten cardiac beats were assisted and hemodynamic data were recorded before the end of 10th cardiac beat to allow the circulation to reach equilibrium before loading a new profile. The simulation was continued for all 343 different profiles which required 3430 cardiac beats. Each profile is then categorized into four distinct triggering algorithms based on the

deflation start and inflation end times: (1) *early deflation late inflation* (ED-LI), (2) *late deflation and early inflation* (LD-EI), (3) *early deflation early inflation* (ED-EI), and (4) *late deflation late inflation* (LD-LI). For example, if deflation start time point is 0.066 and inflation end time point is 0.868 this combination results in *early deflation and late inflation* (ED-LI) algorithm.

Table 7. Control modes for two-segmented counterpulsation device.

HR (BPM)	Time Slots	Early Time Slots			Middle Slot	Late Time Slots		
60	DST	0	0.06	0.13	0.20	0.26	0.33	0.40
	DET / IST	0.40	0.43	0.47	0.50	0.53	0.56	0.60
	IET	0.60	0.67	0.73	0.80	0.86	0.93	1.00
70	DST	0	0.53	0.10	0.16	0.21	0.26	0.32
	DET / IST	0.32	0.35	0.37	0.40	0.42	0.45	0.47
	IET	0.48	0.53	0.58	0.64	0.69	0.74	0.80
100	DST	0	0.04	0.08	0.15	0.16	0.20	0.24
	DET / IST	0.24	0.26	0.28	0.30	0.32	0.33	0.35
	IET	0.36	0.40	0.44	0.48	0.52	0.56	0.60

DST: Deflation Start Time, DET: Deflation End Time, IST: Inflation Start Time, IET: Inflation End Time.

4.3. Data Analysis

4.3.1. Indices of Assistance Effectiveness

Extra-aortic two-segmented CPD assistance effectiveness was accessed through variations in hemodynamic parameters, dynamic pressure (or alternatively KE) enhancement, and LV PV-loops. At every 10^{th} cardiac beat pressure, flow and volume data were recorded to calculate the effect of cuff compliance timing on LV PV-loops and hemodynamic parameters: SV, CO, EF, mean AOF, CAF, aortic systolic and diastolic pressures, MAP, LV peak pressure and ELVW [97]. The dynamic pressure increments were demonstrated through LV PV-loops, and a linear relationship between the CO and percentage increase in the ELVW was established. EDV, ESV, SV, and CO were also determined through PV-loops.

$$MAP = Diastolic\ Pressure + 0.33 * (Systolic\ Pressure - Diastolic\ Pressure) \quad (9)$$

$$ELVW = LV\ Peak\ Systolic\ Pressure - Mean\ LAP * (CO * 13.6 * 9.08 * 0.001) \quad (10)$$

Results are presented as mean ± standard error. Statistical analysis was performed for unequal variances in Matlab 2016b after exporting the data from Simulink. Student t-test was used to compare the mean of hemodynamic parameters of sick heart with all four timing algorithms of extra-aortic two-segmented CPD for 95% confidence interval (significance level = 0.05).

4.4. Results

4.4.1. PV-loop Comparison

LV PV-loops were used to compare the improvement in CO of: a sick heart (no assist); with single cuff assist; two-segmented cuff (filling and ejection optimized using steepest descent method); and optimized two-segmented cuff assist (the best result of achieved using exhaustive search technique). The LV PV-loop for all three cases of HR i.e. 60, 75, and 100 BPM with a LV maximum elastance of (severe to mild HF) 0.5, 0.75, and 1 mmHg/mL respectively, shows that optimized two-segmented CPD has lowered the ESV and lowered the left ventricle ejection pressure (LVEP), resulting in an increased SV as compared to two-segmented cuff and single cuff CPD (Figure 28). However, it can be seen in the LV PV-loops that the filling and ejection profile of optimized two-cuff from exhaustive search produced almost similar improvements (< 2.5% increase in CO) compared to two-segmented cuff CPD profile (presented in (Qureshi et al., 2016)) [95].

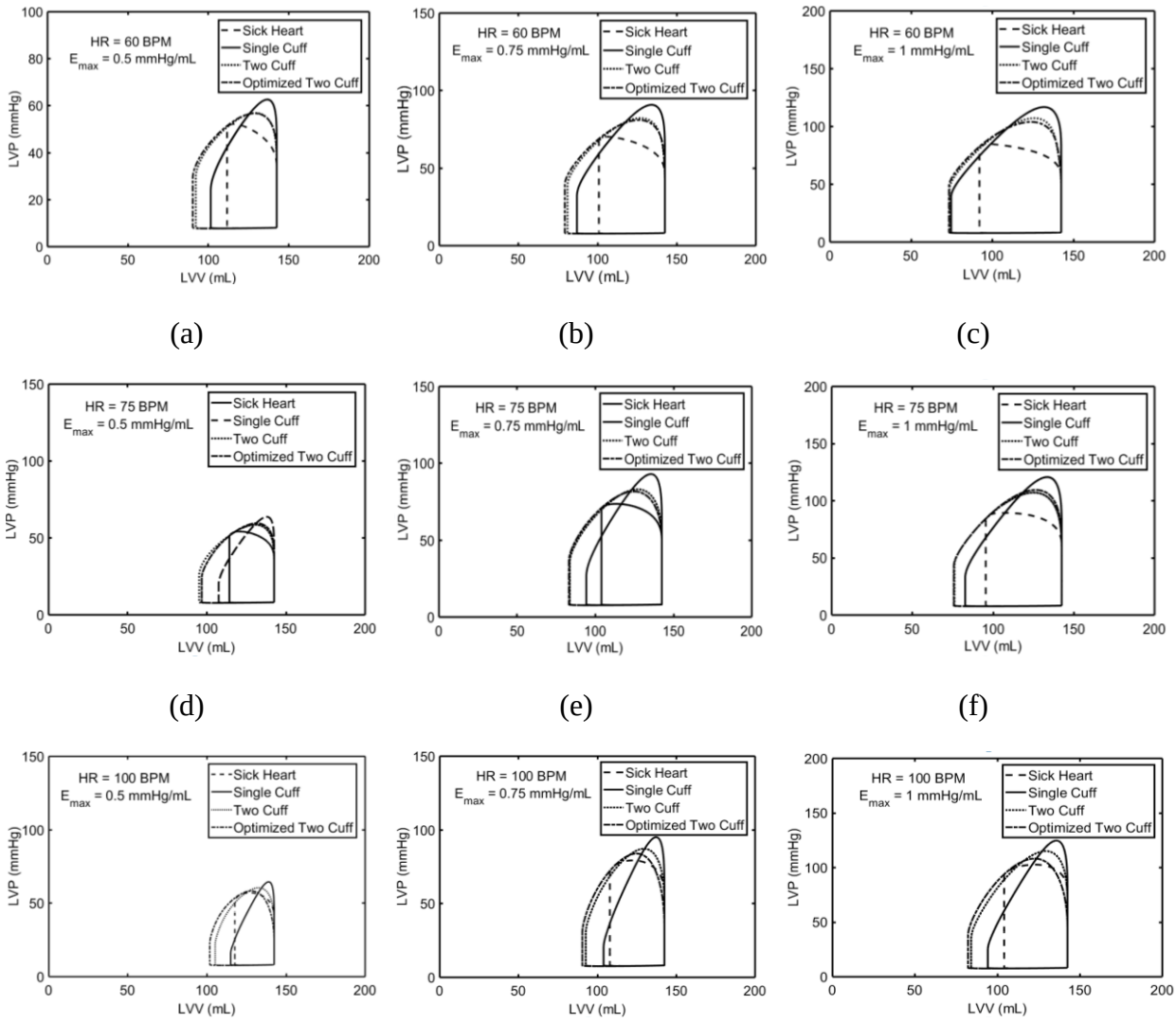

Figure 28. PV-loop comparison of CO increase in optimized two-segmented cuff as compared to sick heart (no assist (baseline)), single cuff and two-cuff, plot (a-b) shows the PV-loop of severe to mild HF for HR of 60 BPM, plot (d-f) shows the PV-loop of severe to mild HF for HR of 75 BPM and plot (g-i) shows the PV-loop of sever to mild HF for HR of 100 BPM. In all three cases optimized two-cuff CPD achieved better SV, decreased peak LVP, and increase EWLV.

4.4.2. Two-Segmented CPD Timing Effect on Hemodynamic

The waveforms of left ventricle pressure (LVP), AOP, AOF, CAF, LV elastance and CPD proximal cuff compliance profile pressure and volume were analyzed for all four timing modes. Figure 29 (a) show a case of severe HF at a HR of 60 BPM where 1st beat in the waveforms corresponds to LD-EI mode, 2nd beat corresponds to ED-LI mode, 3rd beat corresponds to ED-EI

mode, and 4th beat corresponds to LD-LI mode. These 4 beats were chosen out of 343 beats as explained earlier, each CPD profile was set to run for 10 cardiac beats to make sure the CVS system settles down to steady state). It was observed that ED-LI, EE-LI and LD-LI timing modes lowered the LVEP considerably, however, the CO achieved with these timings modes is less as compared to LD-EI mode (Figure 29 (b)).

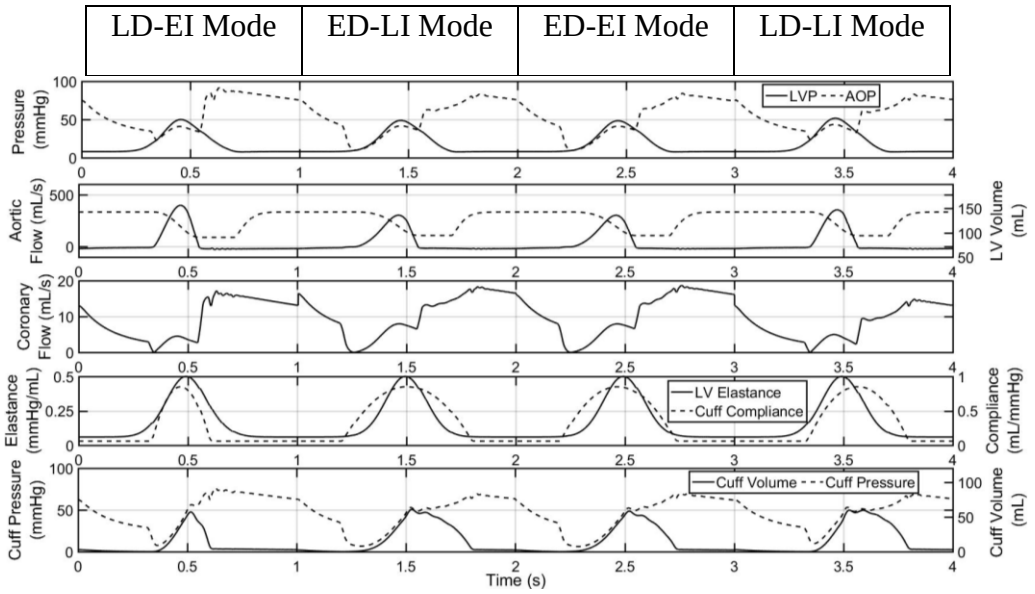

(a)

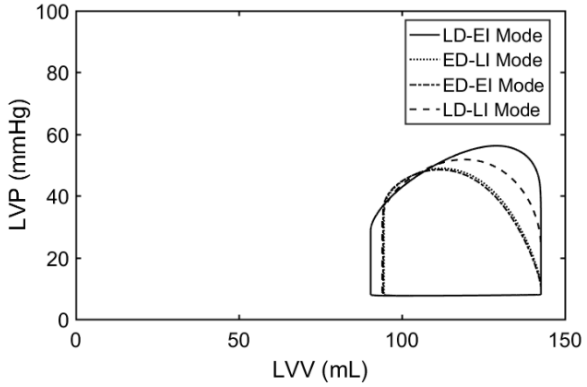

(b)

Figure 29. AOP, LVP, AOF, CAF, LV elastance and CPD compliance, pressure and volume with extra-aortic two-segmented CPD operating in four different timing modes (a): late deflation and early inflation (LD-EI Mode), early deflation and late inflation (ED-LI Mode), early deflation and early inflation (LD-EI Mode), and late deflation and late inflation (LD-LI Mode), while the corresponding PV-loop are shown in (b).

From these plots it is clear that all four timing algorithms provide comprehensive diastolic augmentation and lowered LVEP. However, the corresponding plot PV-loop shows that LD-EI Modes provides a better improvement in CO as compared to ED-LI, ED-EI, and LD-LI Modes which provide greater improvement in lowering LVEP.

The four best compliance profiles of LD-EI timing mode with maximum CO are shown in Figure 30. Figure 30 (a) shows the LV elastance waveform of severe HF with four different LD-EI timings. Figure 30 (b) shows the changes in AOF and LVV with a change in timings of LD-EI mode. The AOF and LVV plots in Figure 30 (b) show similar responses of how AOF was reduce with change in compliance profile timing within a specific mode even. Similarly, the alterations in AOP diastolic augmentation and LVEP (Figure 30 (c)). The corresponding PV-loop (Figure 30 (d)) clearly shows that the changes in CO for similar timing mode are not more than 2.5% however, the compliance profile with symmetrical orientation with LV elastance provides better CO increase. It has also been determined that CO is directly proportional to: 1) dynamic pressure area (DPA) calculated at standard blood density (**ρ**) (Equation (13)), and 2) the percentage increase of EWLW (Equation (14)) shown in Figure 30 (e) and (f) respectively.

$$\text{AOF Velocity} = \text{AOF} / (\text{Area of Aorta}) \tag{13}$$

$$\text{DPA} = 0.5\,(\rho)\,(\text{AOF Velocity})^2$$

$$\text{Total LVP} = \text{LV Static Pressure} + \text{DPA} \tag{14}$$

$$\text{Change} = \text{Area (PV-loop with Total LVP)} - \text{Area (PV-loop with LV Static Pressure)}$$

$$\textbf{\% Increase EWLW} = \textbf{(Change / Area (PV-loop with LV Static Pressure)}$$

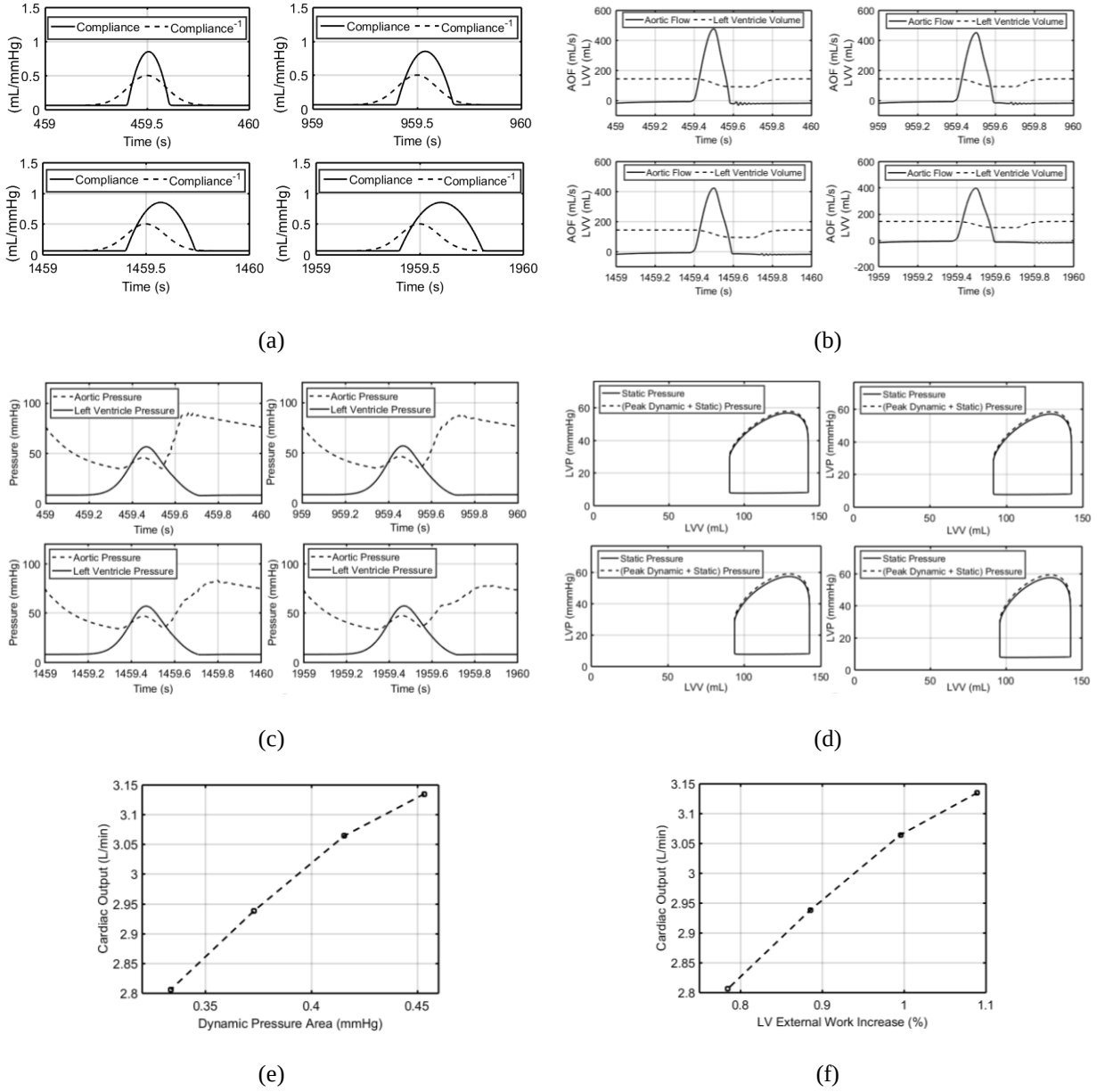

Figure 30. LV elastance, CPD compliance profile (timing mode LD-EI, HR = 60 BPM, and E_{max} = 0.5 mmHg/mL) (a) shows the relationship between the elastance waveform of LV and CPD inflation and deflation timings and their effect on AOF which reduces with increase in time duration between deflation and inflation as shown in (b) which directly affects AOP and LVP waveforms shown in (c), PV-loop shows the increase in ESV and decreases in SV and CO.

Table 8 shows the hemodynamic data of sick heart (no-assist) compared to four timing modes of two-segmented CPD with variations in HR from 60 to 100 BPM and in LV elastance from 0.5 to 1 mmHg/mL. Compared with no-assist ($p < 0.05$) significant improvements were found for all timing modes of two-segmented CPD with increases in SV, CO, EF, AOF, diastolic pressure

augmentation peak (DPA_{peak}), mean coronary artery flow (MCAF) and ELVW and decreases in aortic systolic peak pressure (ASP_{peak}), LVEP, and mean arterial pressure (MAP) as shown in Figure 31.

Table 8. Summary of hemodynamic parameters for no-assist and extra-aortic two-segmented counterpulsation device with the four timing modes.

HR = 78.33 ± 20.20 (BPM) E_{max} = 0.75 ± 0.250 (mmHg/mL)					
No-Assist		Extra-aortic Two-Cuff CPD Assistance			
		LD-EI	ED-LI	ED-EI	LD-LI
SV (mL)	42.3 ± 7.5	54.2 ± 7.8	51.6 ± 5.0	51.8 ± 4.0	51.9 ± 6.5
CO (L/min)	2.9 ± 0.7	4.2 ± 0.8	3.9 ± 0.8	3.9 ± 0.8	4.0 ± 0.9
EF (%)	26.4 ± 6.0	38.0 ± 5.4	35.5 ± 4.4	35.7 ± 4.1	36.0 ± 04.8
AOF_{Mean} (mL/s)	33.7 ± 9.6	48.3 ± 10.5	44.6 ± 12.6	35.9 ± 2.6	47.8 ± 12.0
ASP_{Peak}(mmHg)	77.8 ± 13.7	70.9 ± 19.7	66.2 ± 18.7	62.3 ± 16.3	68.2 ± 17.9
LVEP (mmHg)	53.4 ± 10.3	30.7 ± 12.7	14.5 ± 4.2	11.0 ± 1.9	23.2 ± 9.9
LVP_{Peak} (mmHg)	82.9 ± 14.6	78.7 ± 20.0	75.3 ± 18.6	73.1 ± 18.0	77.2 ± 20.0
MAP (mmHg)	61.5 ± 11.3	44.0 ± 13.5	31.5 ± 8.7	27.9 ± 6.5	38.1 ± 11.02
DPA_{Peak} (mmHg)	53.4 ± 10.3	102.0 ± 13.5	95.6 ± 14.7	85.8 ± 4.3	98.0 ± 13.2
MCAF (mL/s)	2.5 ± 0.6	5.2 ± 0.4	6.8 ± 1.8	6.6 ± 1.0	4.6 ± 0.1
ELVW (J/min)	24.6 ± 12.1	38.3 ± 17.6	33.8 ± 15.6	33.1 ± 15.4	36.1 ± 17.0

All values are expressed as mean ± standard error.

Bigger improvements were recorded for SV with LD-EI (11.89 ± 0.35, 95% CI: 52.49, 56.03) & LD-LI (9.59 ± 0.95, 95% CI: 50.43, 53.49) than with ED-LI (9.23 ± 2.49, 95% CI: 50.22, 52.97) & ED-EI (9.46 ± 3.51, 95% CI: 50.30, 53.35) which ultimately resulted in increased CO and EF respectively. Similarly, compared to no-assist the AOF increase was significant with LD-EI (14.66 ± 0.87, 95% CI: 46.00, 50.73) than that with ED-LI (10.92 ± 2.99, 95% CI: 41.18, 48.07) and LD-LI (14.1 ± 2.39, 95% CI: 45.02, 50.59) but no significant difference between no-assist and ED-EI (P = 0.255). The decrements in ASP_{peak} compared to no-assist were bigger with ED-EI (15.45 ± 2.64, 95% CI: 56.15, 68.59) and ED-LI (11.6 ± 5.08, 95% CI: 61.09, 71.35) than that with LD-LI (9.59 ± 4.27, 95% CI: 64.03, 72.42) and LD-EI (6.87± 6.00, 95% CI: 66.50 75.39).

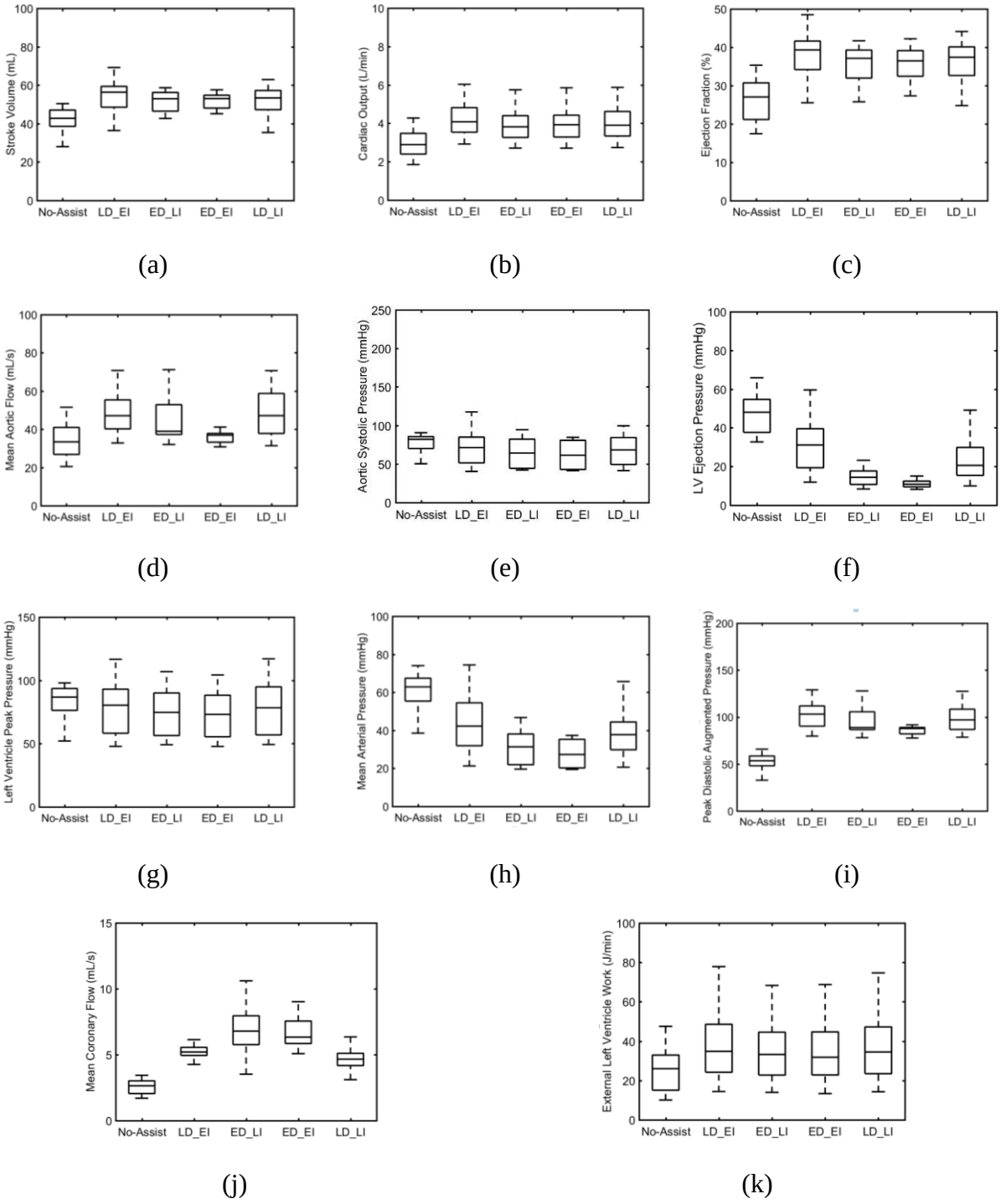

Figure 31. Comparison of changes in no-assist SV, CO, EF, AOF, ASPpeak, LVEP, LVPpeak, MAP, DPApeak, MCAF, and ELVW versus two-segmented CPD timing modes. It is shown that LD-EI timing mode delivers best results for CO increase.

Similarly, compared to no-assist the decrease in LVEP was bigger with ED-EI (42.46 ± 8.44, 95% CI: 10.30, 11.75) and ED-LI (38.98 ± 6.09, 95% CI: 13.34, 15.66) than that with LD-

LI (30.23 ± 0.37, 95% CI: 20.92, 25.58) and LD-EI (22.75 ± 2.38, 95% CI: 27.86, 33.61). Promising reductions in LVP_{peak} compared to no-assist with ED-EI (9.80 ± 3.45, 95% CI: 69.34, 76.95) and ED-LI (7.63 ± 3.98, 95% CI: 71.42 79.22) but LD-EI ($p = 0.148$) and LD-LI ($p = 0.081$) failed to show significance differences. Significant reductions in MAP with all four timings modes compared to no-assist however, bigger reductions with ED-EI and ED-EI than that with LD-LI and LD-EI. Compared to no-assist bigger increments of DPA_{peak} with LD-EI and LD-LI than that with ED-LI and ED-EI. Compared to no-assist all modes significantly increased MCAF with ED-LI being best and LD-EI, LD-LI, and ED-LI showed significant increments with ELVW but ED-EI mode failed to show a significant difference ($p = 0.535$). Figure 32 shows the overall best timing mode (*late deflation and early ejection timing mode)* with arrows indicating the time of deflation and inflation in accordance with LV elastance, LVP, AOP and LVV it can be seen the CPD filling starts at the beginning of the LV systole and ejection starts at the dicrotch notch.

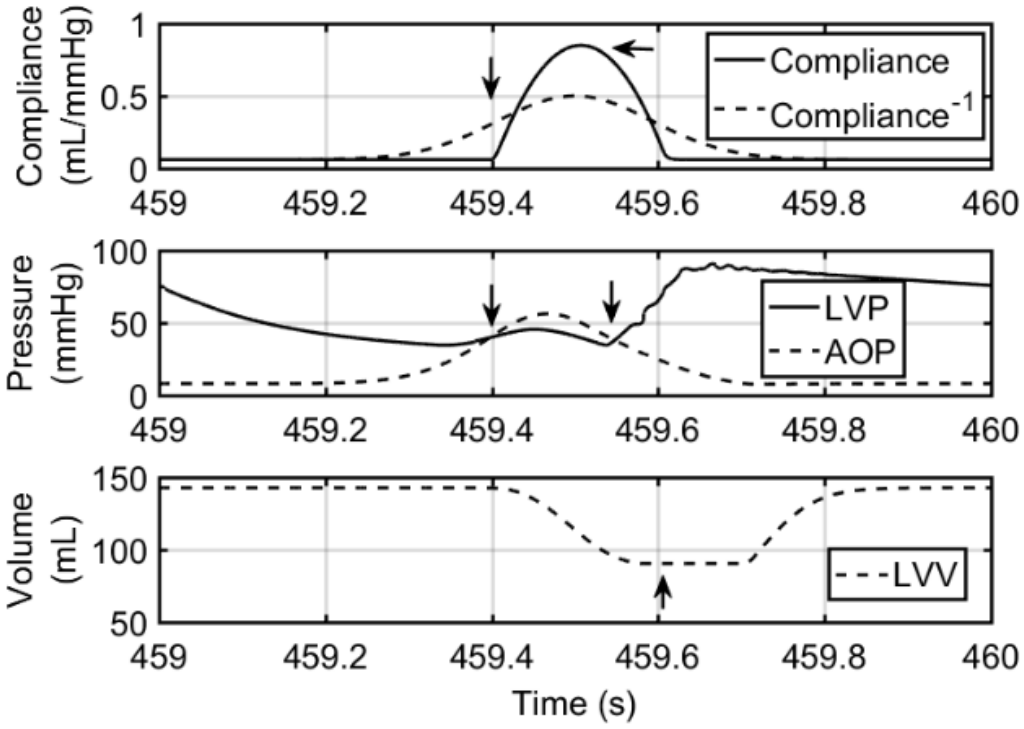

Figure 32. Late deflation and early ejection timing mode with arrows (cuff compliance, LV elastance, LVP, AOP and LVV) indicating the time of filling and ejection of two-segmented CPD.

4.5. Discussion

IABP has become most widely used form of CPD. However, it is limited due to its blood contacting nature, restricts patient mobility, and its potential for limb ischemia. Whereas, extra-aortic CPDs are non-blood contacting, minimally invasive and don't restrict patient mobility. The extra-aortic CPDs are relatively new and are still in clinical trial, however, it has been reported that these devices are incapable of providing sufficient CO for NYHA class III and ambulatory class IV HF patients [10]. Giridharan et al. reported that two counterpulsation devices, one that wraps around the aorta and the other that is anastomosed to the aorta, provided hemodynamic improvements comparable to IABP. During the rapid deflation of MCSDs e.g. IABP/extra-aortic CPD, aortic end-diastolic pressure drops rapidly producing a "steal" phenomena (retrograde blood flow), which limits the amount of diastolic CAF and CO augmentation [87] and Qureshi et al. proposed a two-segmented extra-aortic CPD concept to minimize the retrograde flow and optimize KE of the forward moving AOF [95]. Computer simulation suggested that two-segmented CPD provided better hemodynamic benefits, including increased CO and diastolic coronary augmentation when compared to single cuff CPDs.

The key finding of this study is how variation in deflation and inflation timings of two-segmented CPD affects the hemodynamic parameters. Earlier Giridharan et al. verified CPD with three timing modes: 1) early filling and late ejection (filling before the end of LV diastole and ejection after aortic valve is closed), 2) late filling early ejection (filling is initiated just before the systole and ejection at aortic valve closure, and 3) early filling and early ejection (filling just before the beginning of LV systole and ejection right at the time of aortic valve closure [68]. The simulation results of this study suggested that the early filling and late ejection mode could be more affected as compared to early filling and early ejection in reducing ELVW at the cost of

slightly reduced augmentation in CPD. It has also been reported that shorter filling times reduced ELVW and shorter ejection times lead to diastolic AOP augmentation and increased CAF. Later on Zhang et al. presented a more comprehensive timing algorithms for CPD and reported that in an animal model of the HF, the optimal timing algorithm is filling at the beginning of LV systole and ejection at the end of the isovolumic relation phase [94]. The study also reported that if suboptimal timing algorithm is performed, the advantages of CPD would be diminished or even inverted with more deficiency of LV function, which pointed that timing algorithm for CPD is important for better hemodynamic effects. The results of this study concluded that CPD filling before LV systole leads to a retrograde flow of blood from a distal part of the aorta in Pre-R-wave-deflation and dicrotic notch-inflation and Pre-R-wave-deflation and post-dicrotic notch-inflation mode because the smash between the retrograde and forwarding moving AOF will increase LV afterload. Therefore, the completion of CPD filling instantaneously followed by LV systole can cause severe damage of cardiac function.

In the present study, four timing modes were explored for two-segmented cuff CPD and the data summarized (Table 8) revealed that the optimal timing mode of two segmented CPD is filling at the beginning of systole and ejection at the dicrotic notch, which is similar to the conclusion made by Zhang et al [94]. Ejection of two-segmented CPD after the dicrotic notch (ED-LI timing mode) provides more coronary perfusion and lower LVEP than ejection at the dicrotic notch. However, the result shows that LD-EI mode has the ability to achieve maximum CO increase at the cost of more LVEW which causes slightly higher LVEP and LVP_{peak}.

These computer simulations of two-segmented CPD suggest that timing control and duration of deflation and inflation may allow additional improvement in hemodynamic responses.

In conclusion, the results of optimized two-segmented CPD didn't provide much improvement in CO and out of four timing, *late deflation and early inflation* (LD-EI) showed optimal hemodynamic responses. Future experiments with prototype devices are required to demonstrate the feasibility of the proposed two-segment cuff CPD.

REFERENCES

[1] S. A. Hunt, "Guideline Update for the Diagnosis and Management of Chronic Heart Failure in the Adult: A Report of the American College of Cardiology/American Heart Association Task Force on Practice Guidelines (Writing Committee to Update the 2001 Guidelines for the Evalutation and Management of Heart Failure)," *Circulation*, vol. 112, no. 12, pp. e154–e235, 2005.

[2] J. Butler, G. C. Fonarow, and M. Gheorghiade, "Need for Increased Awareness and Evidence-Based Therapies for Patients Hospitalized for Heart Failure," *Jama*, vol. 310, no. 19, p. 2035, 2013.

[3] E. Braunwald, "The war against heart failure: The Lancet lecture," *Lancet*, vol. 385, no. 9970, pp. 812–824, 2015.

[4] D. Lloyd-Jones *et al.*, "Executive summary: Heart disease and stroke statistics-2010 update: A report from the american heart association," *Circulation*, vol. 121, no. 7, 2010.

[5] V. L. Roger *et al.*, "Heart disease and stroke statistics-2011 update: A report from the American Heart Association," *Circulation*, vol. 123, no. 4, 2011.

[6] V. L. Roger *et al.*, "Heart disease and stroke statistics-2012 update: A report from the American heart association," *Circulation*, vol. 125, no. 1, pp. 2–220, 2012.

[7] L. W. Miller, M. Guglin, and J. Rogers, "Cost of ventricular assist devices can we afford the progress?," *Circulation*, vol. 127, no. 6, pp. 743–748, 2013.

[8] S. Ostenfeld *et al.*, "Prognostic implication of out-of-hospital cardiac arrest in patients with cardiogenic shock and acute myocardial infarction," *Resuscitation*, vol. 87, pp. 57–62, 2015.

[9] S. C. Koenig, P. A. Spence, G. M. Pantalos, R. D. Dowling, and K. N. Litwak, "Development and Early Testing of a Simple Subcutaneous Counterpulsation Device," *ASAIO J.*, vol. 52, no. 4, pp. 362–367, 2006.

[10] P. Solanki, "Aortic counterpulsation: C-pulse and other devices for cardiac support," *J. Cardiovasc. Transl. Res.*, vol. 7, no. 3, pp. 292–300, 2014.

[11] S. M. Hollenberg, C. J. Kavinsky, and J. E. Parrillo, "Cardiogenic Shock," *Ann Intern Med*, vol. 131, pp. 47–59, 1999.

[12] H. J. Hasdai D, Harrington RA, S. M. Califf RM, Battler A, Box JW, and . Deckers J, Topol EJ, Holmes DR, "Platelet Glycoprotein IIb / IIIa Blockade and Outcome of Cardiogenic Shock Complicating Acute Coronary Syndromes Without Persistent ST-Segment Elevation," *J. Am. Coll. Cardiol.*, vol. 36, no. 3, 2000.

[13] J. S. Hochman *et al.*, "Cardiogenic shock complicating acute myocardial infarction—etiologies, management and outcome: a report from the SHOCK Trial Registry," *J. Am. Coll. Cardiol.*, vol. 36, no. 3s1, pp. 1063–1070, Sep. 2000.

[14] H. R. Reynolds and J. S. Hochman, "Cardiogenic shock current concepts and improving outcomes," *Circulation*, vol. 117, no. 5, pp. 686–697, 2008.

[15] F. Zannad *et al.*, "ESC Guidelines for the diagnosis and treatment of acute and chronic heart failure 2012: The Task Force for the Diagnosis and Treatment of Acute and Chronic Heart Failure 2012 of the European Society of Cardiology. Developed in collaboration with the Heart," *Eur. Heart J.*, vol. 33, no. 14, pp. 1787–1847, 2012.

[16] K. G. Malliaras, J. V. Terrovitis, S. G. Drakos, and J. N. Nanas, "Reverse cardiac remodeling enabled by mechanical unloading of the left ventricle," *J. Cardiovasc. Transl. Res.*, vol. 2, no. 1, pp. 114–125, 2009.

[17] H. D. White, R. M. Norris, M. a Brown, P. W. Brandt, R. M. Whitlock, and C. J. Wild, "Left ventricular end-systolic volume as the major determinant of survival after recovery from myocardial infarction.," *Circulation*, vol. 76, no. 1, pp. 44–51, 1987.

[18] J. N. Cohn, R. Ferrari, and N. Sharpe, "Cardiac remodeling-concepts and clinical implications: A consensus paper from an International Forum on Cardiac Remodeling," *J. Am. Coll. Cardiol.*, vol. 35, no. 3, pp. 569–582, 2000.

[19] M. V Cohen, X. M. Yang, T. Neumann, G. Heusch, and J. M. Downey, "Favorable remodeling enhances recovery of regional myocardial function in the weeks after infarction in ischemically preconditioned hearts," *Circulation*, vol. 102, no. 5, pp. 579–583, 2000.

[20] G. F. Mitchell, G. A. Lamas, D. E. Vaughan, and M. A. Pfeffer, "Left ventricular remodeling in the year after first anterior myocardial infarction: A quantitative analysis of contractile segment lengths and ventricular shape," *J. Am. Coll. Cardiol.*, vol. 19, no. 6, pp. 1136–1144, 1992.

[21] J. A. Rumberger, T. Behrenbeck, J. R. Breen, J. E. Reed, and B. J. Gersh, "Nonparallel changes in global left ventricular chamber volume and muscle mass during the first year after transmural myocardial infarction in humans," *J. Am. Coll. Cardiol.*, vol. 21, no. 3, pp. 673–682, 1993.

[22] P. Gaudron, C. Eilles, I. Kugler, and G. Ertl, "Progressive left ventricular dysfunction and remodeling after myocardial infarction. Potential mechanisms and early predictors.," *Circulation*, vol. 87, no. 3, pp. 755–763, 1993.

[23] L. B. Tan, J. E. Jalil, R. Pick, J. S. Janicki, and K. T. Weber, "Cardiac myocyte necrosis induced by angiotensin II.," *Circ. Res.*, vol. 69, no. Ang II, pp. 1185–1195, 1991.

[24] G. Olivetti *et al.*, “Apoptosis in the Failing Human Heart,” *N. Engl. J. Med.*, vol. 336, no. 16, pp. 1131–1141, 1997.

[25] K. T. Weber *et al.*, “Fibrillar collagen and remodeling of dilated canine left ventricle.,” *Circulation*, vol. 82, no. 4, pp. 1387–1401, 1990.

[26] F. J. Villarreal, N. N. Kim, G. D. Ungab, M. P. Printz, and W. H. Dillmann, “Identification of functional angiotensin II receptors on rat cardiac fibroblasts.,” *Circulation*, vol. 88, no. 6, pp. 2849–2861, 1993.

[27] D. G. Kramer, T. A. Trikalinos, D. M. Kent, G. V. Antonopoulos, M. A. Konstam, and J. E. Udelson, “Quantitative evaluation of drug or device effects on ventricular remodeling as predictors of therapeutic effects on mortality in patients with heart failure and reduced ejection fraction: A meta-analytic approach,” *J. Am. Coll. Cardiol.*, vol. 56, no. 5, pp. 392–406, 2010.

[28] C. D. Kontogiannis, K. Malliaras, C. J. Kapelios, J. W. Mason, and J. N. Nanas, “Continuous internal counterpulsation as a bridge to recovery in acute and chronic heart failure,” *World J. Transplant.*, vol. 6, no. 1, pp. 115–124, Mar. 2016.

[29] J. N. Nanas and S. D. Moulopoulos, “Counterpulsation: Historical Background, Technical Improvements, Hemodynamic and Metabolic Effects,” *Cardiology*, vol. 84, no. 3, pp. 156–167, 1994.

[30] T. G. Papaioannou and C. Stefanadis, “Basic principles of the intraaortic balloon pump and mechanisms affecting its performance,” *Asaio J*, vol. 51, no. 3, pp. 296–300, 2005.

[31] R. A. Santa-Cruz, M. G. Cohen, and E. M. Ohman, “Aortic counterpulsation: A review of the hemodynamic effects and indications for use,” *Catheter. Cardiovasc. Interv.*, vol. 67, no. 1, pp. 68–77, 2006.

[32] D. F. Torchiana *et al.*, “Intraaortic balloon pumping for cardiac support: Trends in practice and outcome, 1968 to 1995,” *J. Thorac. Cardiovasc. Surg.*, vol. 113, no. 4, pp. 758–769, 1997.

[33] A. Kantrowitz and A. Kantrowitz, “Experimental augmentation of coronary flow by retardation of the arterial pressure pulse,” *Surgery*, vol. 34, no. 4, pp. 678–687, Oct. 2016.

[34] R. P. Cochran, T. D. Starkey, A. L. Panos, and K. S. Kunzelman, “Ambulatory intraaortic balloon pump use as bridge to heart transplant,” *Ann. Thorac. Surg.*, vol. 74, no. 3, pp. 746–751, 2002.

[35] A. Kantrowitz *et al.*, “Initial clinical experience with a new permanent mechanical auxiliary ventricle: the dynamic aortic patch.,” *ASAIO J.*, vol. 18, no. 1, 1972.

[36] S. D. Moulopoulos, S. Topaz, and W. J. Kolff, “Diastolic balloon pumping (with carbon dioxide) in the aorta—A mechanical assistance to the failing circulation,” *Am. Heart J.*, vol. 63, no. 5, pp. 669–675, 1962.

[37] J. N. Nanas *et al.*, “A vavleless high stroke volume counterpulsation device restores hemodynamics in patients with congestive heart failure and intractable cardiogenic shock awaiting heart transplantation,” *J. Thorac. Cardiovasc. Surg.*, vol. 111, no. 1, pp. 55–61, 1996.

[38] V. Jeevanandam *et al.*, “Circulatory Assistance With a Permanent Implantable IABP: Initial Human Experience,” *Circulation*, vol. 106, no. 12 suppl 1, p. I-183 LP-I-188, Sep. 2002.

[39] S. C. Koenig *et al.*, “Acute Hemodynamic Efficacy of a 32-ml Subcutaneous Counterpulsation Device in a Calf Model of Diminished Cardiac Function,” *ASAIO J.*, vol. 54, no. 6, pp. 578–584, 2008.

[40] S. Mitnovetski *et al.*, “Extra-Aortic Implantable Counterpulsation Pump in Chronic Heart Failure,” 2008.

[41] A. T. Cheung, J. S. Savino, and S. J. Weiss, “Beat-to-beat augmentation of left ventricular function by intraaortic counterpulsation,” *J. Am. Soc. Anesthesiol.*, vol. 84, no. 3, pp. 545–554, 1996.

[42] K. Franco, V. H. Thouram, and M. S. Slaughter, “Counterpulsation Devices for Myocardial Support.”

[43] S. Scheidt *et al.*, “Intra-aortic balloon counterpulsation in cardiogenic shock: report of a cooperative clinical trial,” *N. Engl. J. Med.*, vol. 288, no. 19, pp. 979–984, 1973.

[44] A. A. Lefemine, H. B. C. Low, M. L. Cohen, S. Lunzer, and D. E. Harken, “Assisted circulation. III. The effect of synchronized arterial counterpulsation on myocardial oxygen consumption and coronary flow,” *Am. Heart J.*, vol. 64, no. 6, pp. 789–795, 1962.

[45] H. Bolooki, *Clinical application of intra-aortic balloon pump*, 3rd ed. New York: Futura, 1998.

[46] A. T. Weiss *et al.*, “Regional and global left ventricular function during intra-aortic balloon counterpulsation in patients with acute myocardial infarction shock,” *Am. Heart J.*, vol. 108, no. 2, pp. 249–254, 1984.

[47] M. J. Kern *et al.*, “Enhanced coronary blood flow velocity during intraaortic balloon counterpulsation in critically III patients,” *J. Am. Coll. Cardiol.*, vol. 21, no. 2, pp. 359–368, 1993.

[48] M. Ishihara, H. Sato, H. Tateishi, T. Kawagoe, Y. Muraoka, and M. Yoshimura, “Effects of intraaortic balloon pumping on coronary hemodynamics after coronary angioplasty in patients with acute myocardial infarction,” *Am. Heart J.*, vol. 124, no. 5, pp. 1133–1138, 1992.

[49] W. B. DUNKMAN *et al.*, “Clinical and hemodynamic results of intraaortic balloon pumping and surgery for cardiogenic shock,” *Circulation*, vol. 46, no. 3, pp. 465–477, 1972.

[50] J. N. Bhayana, S. M. Scott, G. K. Sethi, and T. Takaro, “Effects of intraaortic balloon pumping on organ perfusion in cardiogenic shock,” *J. Surg. Res.*, vol. 26, no. 2, pp. 108–113, 1979.

[51] Y. Sugita, H. Emoto, K. Morita, K. Suzuki, and T. Arai, “The effect of intraaortic balloon pumping (IABP) on pulmonary circulation.,” *ASAIO J.*, vol. 31, no. 1, pp. 389–394, 1985.

[52] M. Hilberman, G. C. Derby, R. J. Spencer, and E. B. Stinson, “Effect of the intra-aortic balloon pump upon postoperative renal function in man.,” *Crit. Care Med.*, vol. 9, no. 2, pp. 85–89, 1981.

[53] W. E. Lawson *et al.*, “Improved Exercise Tolerance following Enhanced External Counterpulsation: Cardiac or Peripheral Effect?,” *Cardiology*, vol. 87, no. 4, pp. 271–275, 1996.

[54] D. Williams, K. S. Korr, H. Gewirtz, and A. S. Most, “The Effect of Intraaortic Balloon Counterpulsation on Regional M4yocardial Blood Flow and Oxygen Consumption in the Presence of Coronary Artery Stenosis in Patients with Unstable Angina.”

[55] T. G. Papaioannou *et al.*, “Heart rate effect on hemodynamics during mechanical assistance by the intra-aortic balloon pump.,” *Int. J. Artif. Organs*, vol. 25, no. 12, pp. 1160–1165, 2002.

[56] C. Kao and W. J. Ohley, “Influence of vascular parameters on the effectiveness of intra-aortic balloon pumping: a model study,” *Med. Biol. Eng. Comput.*, vol. 20, no. 5, pp. 529–538, 1982.

[57] K. T. Weber, J. S. Janicki, and A. A. Walker, “Intra-aortic balloon pumping: an analysis of several variables affecting balloon performance.,” *ASAIO J.*, vol. 18, no. 1, pp. 486–491, 1972.

[58] T. G. Papaioannou *et al.*, “Arterial compliance is an independent factor that predicts acute hemodynamic performance of intra-aortic balloon counterpulsation,” *Int J Artif Organs*, vol. 24, no. 7, pp. 478–483, 2001.

[59] C.-Y. Lin, F. T. Galysh, K. J. Ho, and A. S. Patel, “Response to single-segment intraaortic balloon pumping as related to aortic compliance,” *Ann. Thorac. Surg.*, vol. 13, no. 5, pp. 468–476, 1972.

[60] T. G. Papaioannou, D. S. Mathioulakis, J. N. Nanas, S. G. Tsangaris, S. F. Stamatelopoulos, and S. D. Moulopoulos, “Arterial compliance is a main variable determining the effectiveness of intra-aortic balloon counterpulsation: quantitative data from an in vitro study,” *Med. Eng. Phys.*, vol. 24, no. 4, pp. 279–284, 2002.

[61] Y. Sun, “Modeling the dynamic interaction and intra-aortic balloon pump,” 1991.

[62] B. P. Meyns, Y. Nishimura, R. Jashari, R. Racz, V. H. Leunens, and W. J. Flameng, “Ascending versus descending aortic balloon: Pumping: organ and myocardial perfusion during ischemia,” *Ann. Thorac. Surg.*, vol. 70, no. 4, pp. 1264–1269, 2000.

[63] P. S. Freed, T. Wasfie, B. Zado, and A. Kantrowitz, “Intraaortic balloon pumping for prolonged circulatory support,” *Am. J. Cardiol.*, vol. 61, no. 8, pp. 554–557, 1988.

[64] J. D. Manord *et al.*, “Implications for the vascular surgeon with prolonged (3 to 89 days) intraaortic balloon pump counterpulsation,” *J. Vasc. Surg.*, vol. 26, no. 3, pp. 511–516, 1997.

[65] J. J. Schreuder *et al.*, “Beat-to-beat effects of intraaortic balloon pump timing on left ventricular performance in patients with low ejection fraction,” *Ann. Thorac. Surg.*, vol. 79, no. 3, pp. 872–880, 2005.

[66] W. Schraut *et al.*, “Permanent in-series cardiac assistance with the dynamic aortic patch: Blood-prosthesis interaction in long-term canine experiments.,” *Surgery*, vol. 79, no. 2, pp. 193–201, 1976.

[67] J. V Terrovitis *et al.*, “Superior performance of a paraaortic counterpulsation device compared to the intraaortic balloon pump,” *World J. Surg.*, vol. 27, no. 12, pp. 1311–1316, 2003.

[68] G. A. Giridharan, G. M. Pantalos, K. N. Litwak, P. A. Spence, and S. C. Koenig, “Predicted Hemodynamic Benefits Of Counterpulsation Therapy Using A Superficial Surgical Approach,” *ASAIO J.*, vol. 52, no. 1, pp. 39–46, 2006.

[69] G. A. Giridharan, C. R. Bartoli, P. A. Spence, R. D. Dowling, and S. C. Koenig, “Counterpulsation With Symphony Prevents Retrograde Carotid, Aortic, and Coronary Flows Observed With Intra-Aortic Balloon Pump Support,” *Artif. Organs*, vol. 36, no. 7, pp. 600–606, 2012.

[70] C. R. Bartoli *et al.*, “Response to letter to the editor: a novel subcutaneous counterpulsation device: acute hemodynamic efficacy during pharmacologically induced hypertension, hypotension, and heart failure,” *Artif. Organs*, vol. 35, no. 1, pp. 93–95, 2011.

[71] C. R. Bartoli *et al.*, “A novel subcutaneous counterpulsation device: acute hemodynamic efficacy during pharmacologically induced hypertension, hypotension, and heart failure,” *Artif. Organs*, vol. 34, no. 7, pp. 537–545, 2010.

[72] C. S. Hayward *et al.*, “Chronic extra-aortic balloon counterpulsation: first-in-human pilot study in end-stage heart failure,” *J. Hear. Lung Transplant.*, vol. 29, no. 12, pp. 1427–1432, 2010.

[73] M. E. Legget *et al.*, “Extra-aortic balloon counterpulsation: An intraoperative feasibility study,” *Circulation*, vol. 112, no. 9 SUPPL., 2005.

[74] S. Furman, R. Whitman, J. Stewart, B. Parker, and M. McMullen, “Proximity to aortic valve and unidirectionality as prime factors in counterpulsation effectiveness.,” *ASAIO J.*, vol. 17, no. 1, pp. 153–159, 1971.

[75] A. N. Davies *et al.*, “Extra-ascending aortic versus intra-descending aortic balloon counterpulsation—effect on coronary artery blood flow,” *Hear. Lung Circ.*, vol. 14, no. 3, pp. 178–186, 2005.

[76] S. A. Hunt *et al.*, “ACC/AHA 2005 guideline update for the diagnosis and management of chronic heart failure in the adult a report of the American College of Cardiology/American Heart Association Task Force on Practice Guidelines (Writing Committee to Update the 2001 Guidelin,” *Circulation*, vol. 112, no. 12, pp. e154--e235, 2005.

[77] C. T. Starck, J. Becker, R. Fuhrer, S. Sündermann, J. W. Stark, and V. Falk, “Concept and first experimental-RESULTS:-of a new ferromagnetic assist device for extra-aortic counterpulsation,” *Interact. Cardiovasc. Thorac. Surg.*, vol. 18, no. 1, pp. 13–16, 2014.

[78] M. A. Simaan, A. Ferreira, S. Member, S. Chen, J. F. Antaki, and D. G. Galati, "A Dynamical State Space Representation and Performance Analysis of a Feedback-Controlled Rotary Left Ventricular Assist Device," *IEEE Trans Control Syst Technol*, vol. 17, no. 1, pp. 15–28, 2009.

[79] G. a. Giridharan, M. Skliar, D. B. Olsen, and G. M. Pantalos, "Modeling and Control of a Brushless DC Axial Flow Ventricular Assist Device," *ASAIO J.*, vol. 48, no. 3, pp. 272–289, 2002.

[80] D. S. Breitenstein, "Cardiovascular modeling: The mathematical expression of blood circulation," *Master's thesis, Univ. Pittsburgh, PA*, 1993.

[81] Y. C. Yu, "Minimally invasive estimation of cardiovascular parameters," Ph. D. thesis, Univ. Pittsburgh, PA, 1998.

[82] Y.-C. Yu, J. R. Boston, M. A. Simaan, and J. F. Antaki, "Estimation of systemic vascular bed parameters for artificial heart control," *IEEE Trans. Automat. Contr.*, vol. 43, no. 6, pp. 765–778, 1998.

[83] H. Suga and K. Sagawa, "Instantaneous pressure-volume relationships and their ratio in the excised, supported canine left ventricle," *Circ. Res.*, vol. 35, no. 1, pp. 117–126, 1974.

[84] L. Zhong, D. N. Ghista, E. Y. K. Ng, and S. T. Lim, "Passive and active ventricular elastances of the left ventricle," *Biomed. Eng. Online*, vol. 4, no. 1, p. 1, 2005.

[85] Y. Wu, P. E. Allairel, and G. Tao, "An adaptive controller for left ventricle assist device," *in Engineering in Medicine and Biology, 2002. 24th Annual Conference and the Annual Fall Meeting of the Biomedical Society EMBS/BMES Conferece*, vol. 2, pp. 1565–1566, 2002.

[86] Y. Wang and M. A. Simaan, “A New Method for Detecting Aortic Valve Dynamics during Control of the Rotary Left Ventricular Assist Device Support,” *2014 Am. Control Conf.*, pp. 5471–5476, 2014.

[87] W. T. Abraham *et al.*, “Ambulatory extra-aortic counterpulsation in patients with moderate to severe chronic heart failure,” *JACC Hear. Fail.*, vol. 2, no. 5, pp. 526–533, 2014.

[88] R. Yotti *et al.*, “A noninvasive method for assessing impaired diastolic suction in patients with dilated cardiomyopathy,” *Circulation*, vol. 112, no. 19, pp. 2921–2929, 2005.

[89] S. Nakatani *et al.*, “Diastolic suction in the human ventricle: Observation during balloon mitral valvuloplasty with a single balloon,” *Am. Heart J.*, vol. 127, no. 1, pp. 143–147, 1994.

[90] A. Schulz *et al.*, “Preliminary Results From the C-Pulse® OPTIONS HF European Multicenter Post-Market Study,” *Med. Sci. Monit. Basic Res.*, vol. 22, pp. 14–19, 2016.

[91] G. J. Tortora and B. H. Derrickson, *Principles of anatomy and physiology*. John Wiley & Sons, 2008.

[92] D. Randall, W. W. Burggren, K. French, and R. Eckert, *Eckert animal physiology*. Macmillan, 2002.

[93] A. Cheng, G. Monreal, M. L. William, M. Sobieski, and M. S. Slaughter, “Extended Extra-Aortic Counterpulsation With the C-Pulse Device Does Not Alter Aortic Wall Structure,” *ASAIO J.*, vol. 60, no. 6, pp. e5–e7, 2014.

[94] G.-W. Zhang *et al.*, “Optimal Timing Algorithms of Para-Aortic Counterpulsation Device: An Animal Study,” *Asaio J.*, vol. 58, no. 2, pp. 115–121, 2012.

[95] M. B. Qureshi, J. Glower, D. L. Ewert, and S. C. Koenig, “A Novel Idea to Improve Cardiac Output of Mechanical Circulatory Support Devices by Optimizing Kinetic Energy Transfer Available in Forward Moving Aortic Blood Flow,” *Cardiovasc. Eng. Technol.*, 2017.

[96] W. T. Abraham *et al.*, “Reply: Upgrade Ambulatory Extra-Aortic Counterpulsation to Full-Support LVAD,” *JACC Hear. Fail.*, vol. 3, no. 4, pp. 343–344, 2015.

[97] K. D. Reesink *et al.*, “Miniature Intracardiac Assist Device Provides More Effective Cardiac Unloading and Circulatory Support During Severe Left Heart Failure Than Intraaortic Balloon Pumping,” *Chest*, vol. 126, no. 3, pp. 896–902, 2004.